AKENTEN APPIAH-MENKA UNIVERSITY OF SKILL TRAINING AND ENTREPRENEURIAL DEVELOPMENT

SOURCE APPORTIONMENT AND HUMAN HEALTH RISK ASSESSMENT OF POTENTIALLY TOXIC ELEMENTS IN SOILS IMPACTED BY ARTISANAL SMALL-SCALE MINING

EDMUND CRYSTALS OWUSU

2025

AKENTEN APPIAH-MENKA UNIVERSITY OF SKILL TRAINING AND ENTREPRENEURIAL DEVELOPMENT

SOURCE APPORTIONMENT AND HUMAN HEALTH RISK ASSESSMENT OF POTENTIAL TOXIC ELEMENTS IN SOIL IMPACTED BY ARTISANAL SMALL-SCALE MINING, GHANA

EDMUND CRYSTALS OWUSU

8221440002

A thesis submitted to the Department of Chemistry, Faculty of Science, Akenten Appiah-Menka University of Skill Training and Entrepreneurial Development in partial fulfillment of the requirements for the award of a Master of Philosophy degree in Chemistry Education

JULY, 2025

DECLARATION

Student Declaration

I, **EDMUND CRYSTALS OWUSU** declare that this thesis, except for quotations and references in published project works, which have all been identified and duly acknowledged, is entirely my original work, and it has not been submitted, either in part or whole, for another degree elsewhere.

SIGNATURE …….

DATE…….

Supervisor's Declaration

We declare that the preparation and presentation of this work were supervised by the guidelines for supervision of the thesis as laid down by the Akenten Appiah-Mensah University of Skills Training and Entrepreneurial Development.

Supervisor: PROF. KOFI SARPONG

SIGNATURE: ……

DATE: ……

Supervisor: DR. OPOKU GYAMFI

SIGNATURE: ……

DATE: ……

ACKNOWLEDGEMENT

I am very grateful to the Almighty God for His provision of strength, knowledge, and ability to come this far. I would like to express my sincere gratitude to my lecturers and supervisors, Prof. Kofi Sarpong and Dr. Opoku Gyamfi, for their immeasurable support, encouragement, expertise, mentorship, and constructive feedback throughout my thesis journey. Honestly, your commitment to assisting me achieve success in my academic goal remains priceless in my memory.

Again, my reverence and appreciation to Dr. Edward Ankapong, Dr. Eugene Ansah, and all my MPhil colleagues, especially Mr. Lawrence Brenya Kankam, whose enormous contributions led to the success of this work.

DEDICATION

To my lovely wife Ms Matilda Essilfie, my siblings, especially Mr. Charles Owusu, Stella Owusu (Mrs), Faustina Owusu (Mrs.), and my children Lordina Owusu and Gianna Owusu, for their immeasurable support.

TABLE OF CONTENTS

LIST OF TABLES

LIST OF FIGURES

PLATES

ABBREVIATIONS/ACRONYMS/SYMBOLS

APCS	Absolute Principal Component Scoring
ADD	Average Daily Dose
APHA	American Public Health Association
ASGM	Artisanal Small-Scale Mining
ASTM	American Society for Testing and Materials
CCME	Canadian Council of Ministers of the Environment
CF	Contamination Factor
C_{org}	Organic Carbon
CR	Covariance
CRM	Certified Reference Material
DEA	Drug Enforcement Administration
DNA	Deoxyribonucleic Acid
GDP	Gross Domestic Product
GIS	Geographic Information System
DOM	Dissolved Organic Matter
EC	Electrical Conductivity
EF	Enrichment Factor
HHRA	Human Health Risk Assessment
IARC	International Agency for Research on Cancer
ICI	Industrial Combustion Industries
IQ	Intelligent Quotient
Igeo	Index of Geo-accumulation
MCA	Multi-channel Analyzer
MPC	Maximum Permissible Concentration

MLR	Multiple Linear Regression
NEI	National Emissions Inventory
OM	Organic Matter
PCA	Principal Component Analysis
PERI	Potential Ecological Risk Index
PI	Pollution Index
pH	Power of Hydrogen
PTE	Potentially Toxic Element
RfD	Reference Dose
SDG	Sustainable Development Goals
UCL	Upper Confidence Limit
USDA	United States Department of Agriculture
USEPA	United States Environmental Protection Agency
WHO	World Health Organization
OMC	Organic Matter Content
XRF	X-Ray Fluorescence

ABSTRACT

Industrialization and urbanization in developing nations have contributed to the pollution of the biota and the entire ecosystem with potentially toxic elements (PTEs). This study aims to do source apportionment, assess pollution levels, and evaluate the human health risk of PTEs in soil affected by artisanal small-scale mining in the communities of Atwima Mponua District, Ghana. The concentrations of metals and metalloids in 78 soil samples were estimated using a Thermo Scientific field portable Niton X-ray fluorescence analyser. Statistical algorithms, including positive matrix factorization (PMF), principal component analysis (PCA), and various pollution indices, were utilized to apportion the sources, contributions, correlations, and spatial distribution of the PTEs. The mean concentrations of potentially toxic elements (PTEs) in the soil samples were as follows (in mg/kg): mercury (Hg) – 0.304, chromium (Cr) – 2.90, vanadium (V) – 4.47, lead (Pb) – 4.99, arsenic (As) – 9.10, copper (Cu) – 15.47, nickel (Ni) – 26.30, zinc (Zn) – 39.56, titanium (Ti) – 264.00, cobalt (Co) – 121.16, cadmium (Cd) – 204.22, and manganese (Mn) – 361.80. The study found high contamination factors (CF) for Cd (85.10) and Co (2.08). The results of potential ecological risk (PER) for Cd (2553) show very high risk, but that of Co (10.27), and As (3.71) registered low risk. The enrichment factors (Erf) for Cd, Hg, and Co were all > 1.5, indicating significant enrichment in the area. The correlation coefficient analysis showed strong positive correlations between the majority of the PTEs, suggesting common sources. PMF multivariate receptor modelling analysis identified five (5) dominant and sub-dominant source profiles. The results have apportioned source contributions 2,4, and 5 to anthropogenic sources, mainly the artisanal small-scale mining and agricultural activities, and attributed factors 1,3 as both anthropogenic and geogenic sources in the study area. The investigation concludes that the soil in the Atwima Mponua District is at serious risk due to the high levels of PTEs, particularly Cd and Co, which pose significant ecological and human health risks. Hence, policy interventions are necessary to mitigate pollution and protect public health.

CHAPTER ONE

INTRODUCTION

1.1 Background of Study

Soil is a vital component of the environment and is essential for human survival. The health of the ecosystem and society depends on the safety and quality of the soil environment. But in recent years, the increase in industrialization, and urbanization have caused heavy metal(loid)s to accumulate excessively in the soil via different activities like mining, agriculture, combustion, atmospheric droppings, and solid waste disposal. These have resulted in significant soil contamination, with PTEs being the primary contaminants.

Heavy metal contamination of soil is an extremely serious environmental issue, especially when the concentration of the potentially toxic elements (PTEs) in the soil exceeds naturally occurring background levels. Because of their extreme toxicity, bio-accumulation, and persistence, PTEs become highly harmful to both humans and biota. (USEPA, 2024; Fu et al., 2021). PTEs can enter the soil from a variety of sources and include heavy metals such as arsenic, mercury, cadmium, lead, cobalt, titanium, chromium, and cobalt. These substances may persist in the environment and build up in the food chain, endangering the health of the local populace, especially the most vulnerable, the children and expectant mothers (Darko et al., 2017).

Most of the previous studies have primarily focused on agricultural soils. This suggests that few studies have focused on the impacts of practices of artisanal small-scale gold mining and other dispersed companies in Atwima Mponua District. Despite the growing

awareness of pollution risks, there remains a significant knowledge gap regarding the contributions from specific sources of PTE contamination and the extent to which these contaminants affect human health.

The use of receptor models and multivariate statistical analysis techniques in soil pollution source analysis has grown significantly in recent years (Wu et al., 2020). This includes the commonly used multivariate statistical analysis techniques known as principal component analysis (PCA) and absolute principal component scoring-multiple linear regression (APCS/MLR) analysis.

Furthermore, the US Environmental Protection Agency (EPA) advised the implementation of a positive matrix factorisation (PMF) model, which quantitatively estimates the sources of soil PTE contamination by incorporating concentration data and uncertainty analysis. Principal component analysis (PCA), the positive matrix factorisation (PMF) model, and geographic information systems (GIS) have all been used and validated in a reasonable way to successfully identify the main sources of soil heavy metal pollution and determine their contributions. However, previous study analytical methods were ineffective for characterising a particular hotspot since they only examined heavy metal sources of pollution on a regional basis, or over a large area. (Jiang et al., 2017). However, the PMF receptor model analyzes the source contribution of human activity and anthropogenic sources at extremely specific contaminated spots, which could be used to characterize a specific area.

In addition to source identification, this study will carry out a risk assessment for human health (HHRA) to investigate the likelihood of health effects of being exposed to metals and metalloids in the soil. This assessment will take into account various exposure pathways, including ingestion, dermal contact, and inhalation (Asamoah et al., 2023) to provide a comprehensive understanding of the risks faced by the local population. By integrating these methodologies, the goal of the study is to provide insightful and comprehensive information on the environmental and health implications of artisanal small-scale mining in the Atwima Mponua District. The findings will not only contribute to the existing body of knowledge but also inform policymakers and stakeholders in developing effective strategies for risk management and environmental remediation. Ultimately, the research seeks to promote sustainable mining practices that protect both human health and the environment.

1.2 Problem Statement

The World Health Organization (WHO, 2020) states that about one-fourth of the diseases and risks to healthy life facing mankind nowadays are due to prolonged environmental pollution increasing worldwide. The very notable potentially toxic elements are: As, Cd, Co, Cr, Cu, Fe, Hg, Mn, Ni, Pb, Ti, V, and Zn present substantial risks to both environmental and human health. As evidence of unknown specific sources of contributions, several studies have apportioned the heavy metal contaminations to natural and anthropogenic processes (Kumar et al., 2019; Wiafe et al., 2022). According to Sustainable Development Goal (SDG) 15, "Life on Land," we constitute an integral component of the planet's ecosystem, and a healthy life on earth/soil is the basis for our existence.

The extensive utilisation and poor management of soil resources, such as mineral mining, deforestation, loss of natural ecosystems, and land degradation, have caused significant damage to both land and soil. Soil-based activities account for approximately 80% of total water contamination (Country Environmental Analysis, 2020). Polluted soil erosion contributes to the accumulation of plastics, fertilisers, and organic compounds, all of which are harmful to marine ecosystems. Rich soils are being eaten by a chemical degradation process called soil pollution, which may not be plain to the human eye but endangers our food, water, and air (Fisher et al., 2023; Lal et al., 2021).

The vast majority of pollutants originate from human activity and are released into the environment as a result of inappropriate methods of production, use, and disposal, including mining, unsustainable farming, and inadequate waste management. There are no limits to pollution; PTE toxicity permeates food chains through the air, water, and soil and has an adverse effect on both human health and the ecosystem (Kumar et al., 2019; Global Ass. Soil Pollution, 2022).

However, the evidence from the Ghana Chamber of Mines (2019) has brought to bear that about 40% of Ghana's foreign exchange earnings and 5.7% of its GDP come from the mining industry (Ghana Chamber of Mines, 2019). However, all of these advantages come at a high environmental cost, as the extraction and exploitation of gold and other minerals puts stress on the soil and the natural environment, endangering human health (Hadzi, 2017; 2018) and threatening the very human existence.

Despite the economic benefits and risks of ASGM, there is an urgent demand to understand the specific route of all these contaminants and their potential health implications for local communities. Current approaches to soil contamination assessment generally lack the analytical depth required to determine and measure the various sources of PTEs (Alengebawy et al., 2021; Country Environmental Analysis, 2020). Thus, the primary research question guiding this investigation is: What are the predominant sources of PTEs polluting the soil of the Atwima Mponua District, and what are the associated human health risks for the local population? Addressing this question is essential for developing effective policies and practices that mitigate the negative impacts of artisanal mining on both the environment and public health.

1.3 Significance of the Study

This research is extremely important because of the rapid increase in pollution from geogenic and anthropogenic sources in various parts of Ghana. Different works of literature have shown several sources of heavy metal contamination in soil, but not enough studies have apportioned sources of PTEs in soil, assessed heavy metals concentrations and contributions, investigated the human health risk, and proposed appropriate remediation methods to curb the soil pollution in the study area, Atwima Mponua District.

Additionally, assessing PTE sources via the traditional method may inadequately account for the complex interactions among different pollutants and apportion contamination sources (Ahmed et al., 2019). The approaches may lack the analytical depth required to determine and measure the different sources of PTEs.

1.4 Justification

To address the aforementioned gaps, this research combines advanced statistical techniques, Principal Component Analysis (PCA), and Positive Matrix Factorisation (PMF) to facilitate a more nuanced understanding of PTE concentrations, health risks, and apportioned sources in the district's impacted soils. Moreover, comprehensive pollution indices, physicochemical studies, spatial distribution, and human health risk assessment (HHRA) were employed to measure the possible dangers associated with these contaminants, as prior research has frequently ignored this essential component (Armah et al., 2010).

Thus, by incorporating PMF and PCA pollution indices with HHRA, this research intends to provide a clearer picture of the origins and dangers of PTEs in soil, supporting targeted remediation methods and public health initiatives. The results of the study will serve as a basis for tackling the overall soil heavy metal pollution in the country, with a focus on the current PTE contamination level in the selected communities in the Atwima Mponua District. The data would be used to improve government policy and regulatory frameworks to reduce the pollution to the environment and public health posed by PTEs from artisanal and small-scale mining in the Atwima Mponua District. This would help protect the quality of the soil and preserve it for future generations.

1.5 General Objectives of the Study

The study aims to investigate the source and assess the human health risk of potential toxic elements (PTE) in the soil impacted by artisanal small-scale gold mining in the study communities of the purpose of the study is to determine the origin and evaluate the

danger to human health of potential toxic elements (PTE) in the soil that are impacted by small-scale, artisanal gold mining in the Ashanti Region of Ghana. To achieve the aim of the study, these specific objectives would be carried out;

1.5.1 Specific objectives

The study aims to undertake assessments of the Human Health risk of PTE in the soil of Amadaa, Nyinahin, Kukuom, and their neighbouring community mining sites in Atwima Mponua District, Ashanti Region, Ghana.

1. To determine the presence and levels of PTEs (As, Cd, Co, Cr, Cu, Fe, Hg, Mn, Ni, Pb, Ti, V, and Zn) in surface soil samples.
2. To assess the soil sample physicochemical characteristics, including pH, organic matter concentration, and electrical conductivity.
3. To establish the spatial distributions of PTEs within the research location.
4. To predict the source's concentrations and apportion contributions of PTEs in the study area.
5. To assess the risk that PTEs in soils from the research region pose to human health.

1.6 Research Questions

The study will seek to find solutions to the following questions:

1. What is the present state of PTE content in the research area's soils?
2. How would the variation in physico-chemical parameters like pH, organic matter content, and electrical conductivity affect the transfer of PTE in soil?
3. What is the PTE spreading pattern in the research area?

4. What are the sources, concentrations, and proportional contributions of potentially toxic elements (PTEs) in the study area.
5. What levels of human health risk do these PTEs pose to exposed populations?

1.7 Study Organization

The research project is organised into five chapters. The first chapter presents a brief overview and background for the study. The chapter explains the study's goal and specifies the basic terms related to illegal mining. Chapter 2 examines the existing literature on illegal mining in Ghana. It also provides a historical perspective on gold mining in Ghana, focusing on the actions of illicit miners in the Ashanti and Western regions. Chapter 3 focuses on the material and methods employed in this study. Chapter 4 examines the findings of the pollution indicators, the sources allotment, and the potential risks to human health posed by artisanal small-scale mining in Ghana, while Chapter 5 summarises the important findings, conclusions, and recommendations offered.

CHAPTER TWO

LITERATURE REVIEW

2.1 Potentially Toxic Elements in Soil Samples

Concerning potentially toxic elements (PTE), several studies have given different interpretations. Another way to conceptualize potentially toxic elements (PTEs) as heavy elements is that they are considered a subset of elements with element characteristics. It consists of actinides, lanthanides, and transition elements (Alengebawy et al., 2021).

According to Suciu et al. (2008), some people classified potentially toxic elements (PTEs) of heavy metals as having a specific density of more than 5 g/cm^3. They may also be found in a variety of soils, rocks, and water in freshwater and terrestrial environments at concentrations higher than 4 g/cm^3 (Alengebawy et al., 2021). Any relatively dense material that is harmful or poisonous, regardless of its small amounts, is considered a heavy metal.

A chemical element is considered a heavy metal if its specific gravity is at least 5 times higher than that of water. Another school of thought defines potential toxic elements (PTE) of heavy elements as occurring naturally in rock. Compared to the average particle density of soils, which is 2.65 g/cm3, these elements have a density of 6.0 g/cm3 or greater (Country Environmental Analysis, 2020) Thus, potential toxic elements (PTEs) refer to the group of heavy elements that have a toxic potency to accumulate and pollute the environment and risk human health.

2.2 Source and Distribution of Potential Toxic Elements (PTEs)

Table 2.1 Anthropogenic and natural sources of Potential Toxic Elements

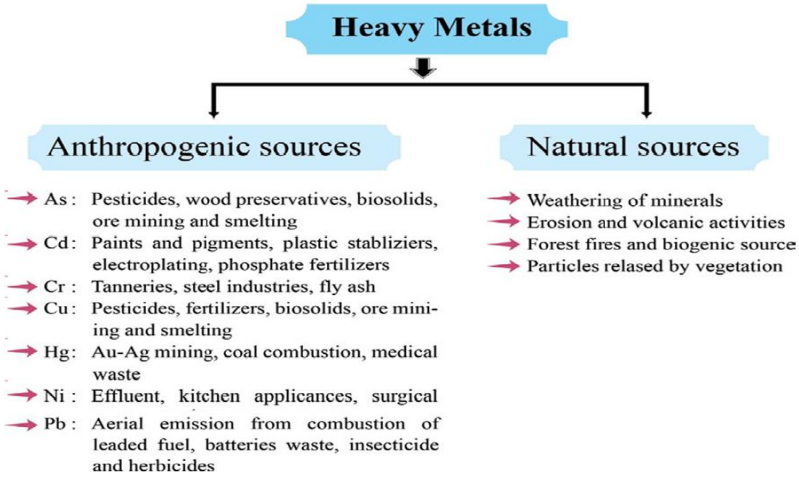

(Delower Hossain et al., 2020)

The main sources of heavy metal(loid)s pollution in soil include different types of mining, manufacturing, burning, and the use of pesticides. The source, or the actual place where the heavy element comes from (such as a factory or wastewater treatment plant), should be taken into account initially. The process by which a heavy element is moved from its source to its destination is known as the dispersion and deposition mechanism (Hadzi, 2017). The total content of PTEs is the average concentration of elements derived from minerals in the geological parent material that the soil has developed on, as well as inputs from a variety of potential anthropogenic sources (Alloway, 2013). Heavy toxic elements are frequently found in soil via the deposition of small aerosol particles (less than 30 mm in diameter) in the atmosphere, heavy element-containing raindrops, direct

applications of fertilisers and agrichemicals, and other organic materials like composts, animal manures, sewage sludges, and food debris (Polissar et al., 1998).

Table 2.2 Emission source and marking elements

Emission Source (Profile)	Source Signatures / Elements
Au-Ag mining	Hg, Cd, As, Mn, C, NO_3^- CN, Sr,
Soil	Al, Si, Sc, Ti, Fe, Sm, Ca
Road dust	Ca, Al, Sc, Si, Ti, Fe, Sm
Sea Salt	Na, Cl, Na^+, Cl^-, Br, I, Mg, Mg^{2+}
Oil burning	V, Ni, Mn, Fe, Cr, As, S, $SO_4^{2-,}$
Coal burning	Al, Sc, Se, Co, As, Ti, Th, S
Iron and steel industries	Mn, Cr, Fe, Zn, W, Rb
Non-ferrous element industries	Zn, Cu, As, Sb, Pb, Al
Glass industry	Sb, As, Pb
Cement Industry	Ca
Refuse incineration	K, Zn, Pb, Sb
Automobile gasoline	Cele, Br, Ce, La, Pt, $SO_4^{2-,}$ NO_3^{2-}
Straw burning	K, C, Br,
Automobile diesel	C, SO S
Secondary aerosols	$SO_4^{2-,}$ NO_3^{2-}, NH_4^+

(Brown et al., 2015; Delower Hossain et al., 2020)

2.3 Physical and Chemical Properties of the Heavy Elements

Heavy metals and metalloids can also be classified as pollutants in the soil environment. Geogenic activities accelerate the release of PTEs into the environment (Zhang et al., 2021), while the elements' chemical properties determine how readily they migrate, persist, and bioaccumulate (Fashola et al., 2016). For instance, mining introduces As and Pb directly into soils, where their solubility under acidic conditions increases their entry into groundwater and crops (Ali et al., 2019). Similarly, industrial Hg emissions are distributed globally due to its volatility where human Activities is primary sources (Naqvi et al., 2022). Agricultural practices contribute significantly, with phosphate

fertilizers introducing Cd and Pb, pesticides adding As and Hg, and animal manure enriching soils with trace metals (Nagajyoti et al., 2010). Industrial emissions from fossil fuel combustion, electroplating, and cement production distribute V, Cr, and Ti via atmospheric deposition, while urbanization, sewage sludge disposal, and e-waste recycling elevate Cu, Pb, and Hg in soils (Ali et al., 2019). Transportation further adds Pb, Cu, and Zn through fuel combustion, tire wear, and lubricants. Naturally occurring elements of the Earth's crust, heavy elements are often not biodegradable and cannot endanger environmental life. According to Adedinola et al. (2009), living things that live in contaminated locations are exposed to exceptionally high levels of heavy metals. Although it can help with water shortages, irrigation with sewage effluent can potentially introduce heavy metals and cause environmental issues.

In addition to other sources, Adelekan and Abegunde (2011) claim that ingesting, breathing, skin contact, or absorption are the ways that heavy metals may enter the human body. Additionally, they build up in aquatic biota, plants, and soils. Various organic and inorganic colloids can contain heavy elements that remain available to living organisms for a long period. They do not lose their potency over time because they are not biodegradable. It can become biomagnified if an organism gets rid of heavy materials more slowly than it takes them in. Because of this, they could be dangerous to both people and animals. Their densities are also comparatively high. Heavy elements are found close to the bottom of the periodic table, in addition to having large densities. Due to their lengthy biological half-lifetimes, heavy elements bioaccumulate and might be hazardous. Additionally, they exist as cations that have a significant interaction with the soil matrix (Rajaganapathy, 2011).

2.3.1 Soil Characterization

The inorganic ligands, mineral phases, pH, organic matter content, organic carbon content, and oxides are some of the chemical and physical properties of soil that significantly influence the mobility of heavy metals in soil (Asamoah et al., 2021). Chemical reactions occurring on the oxide surfaces, such as the bioavailability of nutrients in soils and the behaviour of heavy metals. Organic matter has been recognised to be the dominant soil constituent for lowering the concentration of free elemental ions in soils and their solutions. But the distribution of heavy metals in soil is determined by their interactions with organic materials (Mkhize, 2020). To investigate the effects of dissolved organic matter (DOM), scientists introduced Cd and Zn sorption to acidic, calcareous clay loam and calcareous sandy loam soils. Basically, due to its low clay content, they discovered that calcareous sandy loam retained fewer elements than loam, compared to loam; however, it also demonstrated more potent hindering effects on zinc sorption.

Both the physical and chemical characteristics of elements in soil have a significant impact on the mobility and fate of heavy metals in the soil. Using a Jenway pH and conductivity meter probe (Model 3540, Stone, Staffordshire, UK), the electrical conductivity and pH of the soil samples would be determined. For the measurements in the 1:2 dry soil distilled water mixes, 40 mL of distilled water would be mixed with 20 g of the sieved soil sample. The pH and electrical conductivity of the soils would be assessed one hour after the suspension of water and soil particles had settled. However, the 2 main ways that soils retain heavy elements are by adsorption processes that create complexes with the surfaces of organic materials, oxides, and clays, and precipitation

reactions that produce insoluble precipitates such as hydroxides, carbonates, and phosphates (Mkhize, 2020).

2.4 Health Effects of PTE Exposure on Humans

Ingestion, inhalation, and skin contact are common pathways through which people are exposed to potentially harmful substances in soil. The digestive system is used for ingestion, the respiratory system is used for inhalation, and the skin is used for dermal absorption (Moni et al., 2023). The degree of exposure along a certain pathway is indicated by the liquid, gas, solid-state, or chemical form in which potentially hazardous compounds are present (Jaishankar et al., 2014). Inhaling airborne toxic substances and soil particles spread throughout the environment is the primary way that people are exposed to them (USEPA, 2017). The potential consequences of breathing potentially hazardous elements are influenced by the volume, force, and degree of inspiration, the exposed person's age and sex, and the organ implicated (oral or nasal) (USEPA, 2017).

The body may be harmed by inhaling airborne contaminants like arsenic, cadmium, lead, nickel, and other harmful substances. Potentially toxic substances attract the attention of a large number of researchers since they are released into the environment in trace amounts, and it takes a while for the effects to manifest in the exposed population. The forms in which potentially risky substances are found in the environment dictate how poisonous they are to biological systems, according to research (Ali et al., 2019). PTEs can be found in metallic, inorganic, and biological forms. For example, it is commonly recognized that lead, arsenic, and mercury are less harmful in their inorganic forms than in their organic ones. The amount of potentially poisonous substances absorbed by the

skin can be measured by the exposed surface area and the dermal absorption factor of each metal (Mitra et al., 2022). Therefore, all exposure pathways allow a significant amount of potentially harmful elements to enter the exposed person's body, even though the amount may differ from one exposure pathway to another (Balali-Mood et al., 2021).

Increased levels of potentially hazardous substances significantly impair the body's ability to carry out physiological processes like nerve transmission and metabolism. Additionally, they have the potential to cause cancer, harm internal organs and systems, and possibly cause death. The following metals are examples of potentially dangerous metals that are known to be stable and not able to be broken down or digested by the body: lead, zinc, copper, cadmium, chromium, nickel, and mercury. Once they build up in the body's tissues, organs, and bones, these potentially dangerous compounds start to have negative effects (Witkowska et al., 2021). The human body can only withstand potentially hazardous substances within the prescribed limit (Mihankhah et al., 2020). Occasionally, both acute and chronic symptoms are observed following exposure to a higher concentration of potentially hazardous substances. Chronic toxicity, which is associated with extended exposure to potentially harmful compounds, is usually the form of toxicity most pertinent to environmental toxicants (Javaid et al., 2022).

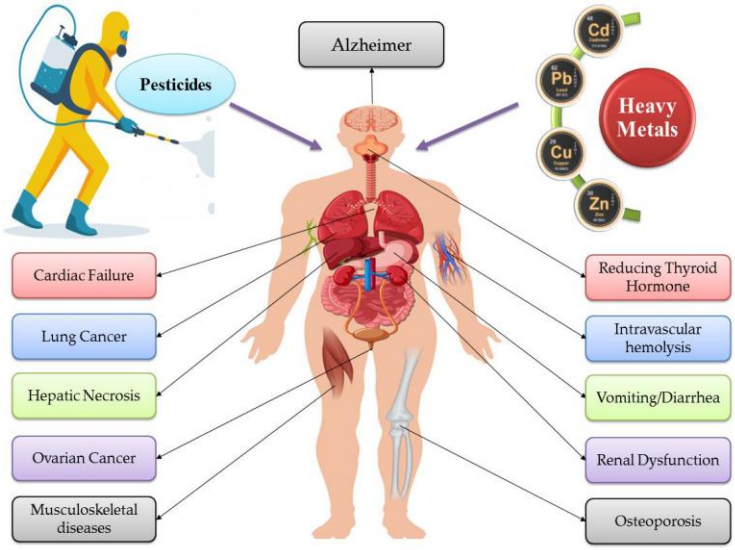

Figure 2.1 Impact of Heavy Metals on Human Health (Alengebawy et al., 2021)**.**

2.5 Toxicity Effects of Selected Potential Toxic Elements (PTEs)

Heavy metal(loid)s that were to be identified in the samples of the soil were: arsenic (As), cadmium (Cd), cobalt (Co), copper (Cu), chromium (Cr), iron (Fe), lead (Pb), mercury (Hg), manganese (Mn), nickel (Ni), vanadium (V), Zinc (Zn).

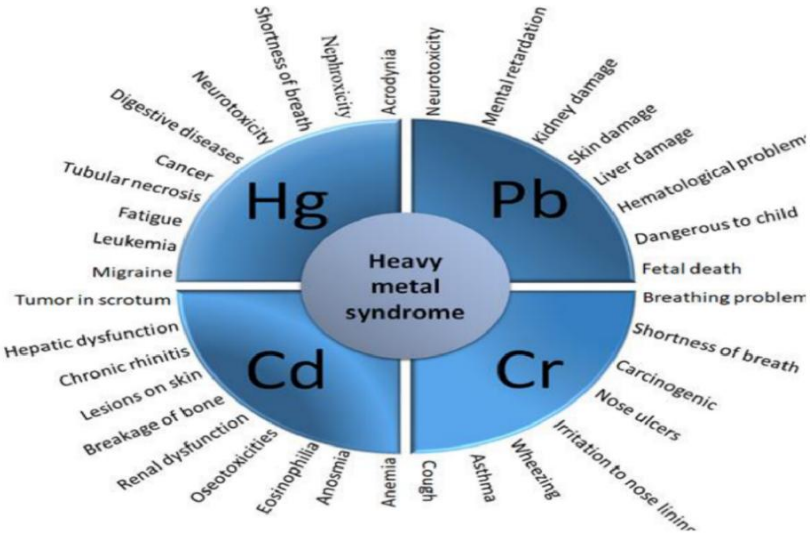

Figure 3.2. Health risks caused by mercury, lead, cadmium, and chromium in the human body (Delower Hossain et al., 2020;Naqvi et al., 2022)

Epidemiological investigations established several possible threats posed by potentially harmful elements in body contact, which must be reviewed. In this review, the study will focus on physiological diseases and mechanisms associated with the dangerous consequences of heavy elements present in soil.

2.5.1 Toxic effects of exposure to Zinc

Major increases in zinc are the result of industrial activities, including gold mining, coal mining, steel manufacture, waste, and combustion. Additionally, from the application of fertilisers, insecticides, liquid manure, composted materials, and fertilisers in agriculture. According to Hardy et al. (2008), it is utilised in the manufacturing of paint, dye, rubber, wood preservatives, and ointments. Because of its high concentration in industrial plant

effluent, zinc (Zn) may pollute the water table and other bodies of fresh water due to its water-soluble forms in soil. This could make the water more acidic, which might harm earthworms and microbial activity, delaying the decomposition of organic compounds.

2.5.2 Toxic effects of exposure to Chromium (Cr)

The sources of Cr contamination include disposal that contains Chromium (IV) and discharges from electroplating operations. Coal combustion and industrial activities also contribute to Cr in soil. The type of Cr (VI) that is typically found in contaminated sites has dangerous levels, and they are frequently found in the soils treated with sewage (Wuana and Okieimen, 2011; Asio, 2009). Organic materials in the soil can decrease it to Cr (III) (Wuana and Okieimen, 2011). In its soluble or precipitated form, it can be transported to surface waterways by surface runoff. The majority of chromium (Cr) that is discharged into natural waters is linked to particles and ends up in sediment. The metabolism of carbohydrates and fats, the use of amino acids, paints, cement, rubber, element plating to prevent corrosion, tanning leather, and textile colour pigments all require chromium (Cr). Furthermore, according to Bhagure and Mirgane (2010), it helps to maintain a normal glucose tolerance factor. Human allergic dermatitis, gastrointestinal haemorrhage, respiratory tract cancer, and skin ulcers can all result from chromium (Cr) exposure. Additionally, mucous membrane injury, liver damage, and renal damage are mentioned (Sako & Nimi, 2018).

2.5.3 Toxic effects of exposure to Copper (Cu)

High levels of copper (Cu) can lead to anaemia, hypertension, neurological problems, liver, kidney damage, irritation of the stomach and intestines. soil component cannot

break down copper and allow it to bioaccumulate in the food chain (Liu et al., 2023). It can also be defined as a poisonous waste that is unfit for human consumption (Nduka et al., 2023).

2.5.4 Toxic effects of exposure to Cadmium (Cd)

Cadmium is used in a variety of products, such as Ni/Cd batteries, pigments, PVC stabilisers, TV manufacture, amalgam in dentistry, anticorrosive coatings for components, and worm treatments for pigs and poultry. air pollution, industrial waste disposal, the use of pesticides, motor oil, sewage sludge, fertilisers, and biosolids (sewage sludge) as well as the application of agricultural inputs.

Kidney failure is the 1st sign of cadmium poisoning, followed by cardiovascular disease, renal problems, severe joint pain, kidney and lung problems, and anaemia due to decreased iron absorption by the intestines. According to Adelekan and Abegunde (2011), an impact on sperm lowers birth weight and is a contributing factor to cardiovascular illnesses and high blood pressure. According to Bhagure and Mirgane (2010) claims that, conditions like liver malfunction, brain damage, hypertension, carcinogenicity, teratogenicity, nausea, vomiting, cramping, and loss of consciousness are all brought by cadmium. Cadmium is the seventh most dangerous heavy metal according to the ATSDR assessment. It is a by-product of zinc production that humans and animals may encounter in the workplace or in the environment. This element will build up inside the human body over a period of time once it is absorbed. During World War I, this element was initially employed as a tin substitute and as a pigment in the paint industry (Jaishankar et al., 2014). In the modern world, it is also found in tobacco smoke,

rechargeable batteries, and the manufacturing of specific alloys. Cadmium is utilised as an electrode component in alkaline batteries to a degree of around three-fourths; the remainder is utilised as a plastic stabiliser and in coatings, pigments, and plating. Humans may be exposed to this element mainly through ingestion and inhalation, and they can develop both acute and long-term toxic exposure (Jaishankar et al., 2014).

2.5.5 Toxic effects on exposure to Lead (Pb)

A buildup of lead (Pb) in the body's organs, such as the brain, can cause poisoning (plumbism) or potentially cause death. The central nervous system, kidneys, and gastrointestinal tract may all be impacted by lead (Pb) exposure. Lead (Pb) exposure, for example, causes developmental delays, decreased IQ, attention deficit disorder, hyperactivity, and mental decline in children. Asiminicesei et al., (2020) have identified children under six as being particularly vulnerable. Adults exposed to lead experience decreased reaction time, memory loss, nausea, insomnia, anorexia, joint weakness, infertility, haemoglobin synthesis suppression, irritation, and tumour development Asio, (2009).

2.5.6 Toxic effects of exposure to Cobalt (Co)

Exposure to cobalt can occur from both natural and man-made sources. Natural sources include wind-borne dust, sea spray, volcanic eruptions, forest fires, and biogenic emissions from the sea and the continent. The mining and smelting of cobalt ores, the processing of cobalt alloys, the burning of fossil fuels, sewage sludge, phosphate fertilisers, and other businesses that utilise or process cobalt compounds are examples of anthropogenic sources (Armah et al., 2010). Cobalt settles on soil when injected into the

atmosphere, although it can either sorb directly to sediment in water or bind to particles and settle there. Among its many uses are electroplating, magnetic steels, alloys for gas turbines and jet engines, and ground coatings for porcelain enamels. Because it is a component of vitamin B12, which is vital for human health, cobalt is significant for humans (Bhagure and Mirgane, 2010). Lentech (2012) states that people can get bronchial asthma, interstitial lung disease, lung cancer, pneumonia, heart issues, thyroid damage, nausea, vomiting, and diarrhoea if they inhale or come into contact with cobalt via their skin. Animals' development and ability to reproduce may then be impacted by cobalt exposure.

2.5.7 Toxic effects of exposure to Nickel (Ni)

State that element plating, burning fossil fuels, nickel mining, and electroplating are the main causes of nickel contamination in soil. Exposure to nickel (Ni) can also happen through inhalation, drinking water, and contaminated food. After passing through precipitation reactions, it falls to the land after being discharged into the atmosphere by power plants and waste incineration facilities. Nickel can also enter surface water as a by-product of wastewater streams. According to Asia (2009), Ni applications include the manufacturing of stainless steel, coinage, nickel for armour plates, vegetable oils, ceramics, burglar-proof vaults, and Ni-Cd batteries. Nickel may damage the lungs, liver, and kidneys. Additionally, allergic responses, dermatitis, eczema, heart failure, respiratory failure, cancer, birth defects, and nervous system issues can all be brought on by high Ni levels (WHO Global Strategy on Health, Environment and Climate Change, 2020; Asio, 2009).

2.5.8 Toxic effects of exposure to Manganese (Mn)

The coal-fired brickfield operations are the potential source of Mn in the soil (Hossain Bhuiyan et al., 2021). Besides, the leather tanning industry releases a considerable amount of Mn into the soil as a source. The iron and steel industries are major contributors of Mn to the environment. (Ali et al., 2019b). Despite being a necessary metal for the body, manganese only recently gained attention due to the introduction of the gasoline additive methylcyclopentadienyl manganese tricarbonyl (MMT), which was recognized to be hazardous (Tawabini et al., 2023). MMT is a manganese exposure in the workplace that has purportedly been linked to the development of a Parkinson's disease-like condition marked by tremors, irregular gait, postural instability, and cognitive impairments. (Kabir & Rashid, 2022; Nkansah et al., 2017; Tawabini et al., 2023). Neurotoxicity may develop from prolonged exposure to high manganese levels (Mkhize, 2020). Manganism, a neurological disorder caused by manganese, is typified by stiffness, movement tremors, a mask-like expression, difficulties with walking, bradykinesia, micrographia, mood issues, and memory and cognitive failure. In terms of symptoms, manganism and Parkinson's disease are similar in a number of ways (Delower Hossain et al., 2020; Mkhize, 2020).

2.5.9 Toxic effects of exposure to Arsenic (As)

Arsenic is one of the most important heavy metals that are problematic from an ecological and individual health standpoint due to its semi-metallic nature, high toxicity and carcinogenicity (Fashola et al., 2016) and broad availability as oxides, sulphides, or as a salt of iron, sodium, calcium, or copper (Jaishankar et al., 2014). The elevated Irrigation and arsenic-contaminated groundwater can contribute to soil accumulation.

Arsenic exposure in humans can occur via industrial processes, natural processes, or unexpected sources. Natural mineral deposits, arsenical pesticides, and improper disposal of arsenical compounds can all pollute drinking water (Fashola et al., 2016). Acute poisoning can also occur from inadvertent consumption by youngsters or intentional administration during suicidal attempts.

According to Jaishankar et al. (2014), arsenic is a proto-plastic toxin since it mostly damages the sulphydryl group of cells (Jaishankar et al., 2014), which results in abnormalities in mitosis, respiration, and enzymes. Pesticide and aerosol deposition in the atmosphere may be a factor in the accumulation of pollutants in the research area's soils. Arsenic's carcinogenic toxicity is characterised by stages. According to Jaishankar et al., (2014) the initial stage is characterised by gastrointestinal symptoms as vomiting, diarrhoea, and bleeding. Within six to twenty-four hours after an overdose, there is a latent phase of apparent medical recovery before the second stage begins.

The third stage, which is characterised by hypotension, shock, lethargy, hepatic necrosis, tachycardia, and metabolic acidosis Lal et al., 2021) begins 12 to 96 hours after the onset of clinical symptoms and frequently ends in death (Mkhize, 2020). The fourth and last stage typically takes place between two and six weeks. This stage is characterised by the development of gastrointestinal ulcers and strictures (Jaison & Muthukumar, 2017).

People with high As concentrations are more likely to get cancer (Alengebawy et al., 2021). Regular asbestos exposure increases the risk of developing asbestosis, which is known to cause lung cancer, as asbestos contains around 30% As (Jaison & Muthukumar,

2017). Jaison & Muthukumar, (2017). Free radicals are thought to be the cause of asbestos-related cancer, and there is evidence that arsenic creates them. DNA oxidation and damage caused by arsenic-generated free radicals can result in serious cancer (Fashola et al., 2016b).

2.5.10 Toxic effects of exposure to Iron (Fe)

Iron is essential for the growth and survival of almost all living organisms. According to Jaishankar et al., (2014);Vuori, (1995) it is an essential component of oxygen-transporting proteins like haemoglobin and myoglobin, as well as of organisms like algae and enzymes like cytochromes and catalase. For many biological redox processes, iron is a desirable transition metal because it can interconvert between ferrous (Fe3+) and ferric (Fe3+) ions. The anthropogenic source of iron in surface soil is associated with mining operations (Jaishankar et al., 2014). Iron pyrites (FeS2), which are frequently found in coal seams, oxidise, producing sulphuric acid and releasing ferrous (Fe3+). The deep ocean typically contains 0.6 nM, or 33.5×10^{9} mg/L, of dissolved iron. Groundwater has a relatively high concentration of dissolved iron (20 mg/L), while freshwater has a very low content (5 μg/L-ICP) (EPA, 1993).

According to the European Union Directive 98/83/EC on the quality of drinking water, many individuals in countries like Lithuania have been shown to have increased amounts of iron through their drinking water since the collected groundwater exceeded the permissible limit (Grazuleviciene et al., 2009). Iron pollution has both direct and indirect impacts that significantly impact fish variety, benthic invertebrate diversity, and periphyton abundance. Through its blocking effect, the iron precipitate will seriously

impair fish respiration (EPA, 1993). A dose of 1 mg/L total iron inhibited the development of aquatic reed species, according to a study on iron toxicity in aquatic plants, especially rice (Phippen et al., 2008). When zinc deficits and acidic soils coincide, wetland rice experiences a macronutrient imbalance. Lowland rice production was significantly impacted by the flooded soils' lower iron (Fe3+) concentrations. Acropetal translocation into leaves, bronzing of rice leaves, higher absorption of Fe3+ by roots, and yield loss are the hallmarks of iron toxicity in rice (Becker & Asch, 2005).

2.5.11 Toxic effects on exposure to Mercury (Hg)

The main human activities that contribute to mercury pollution include mining, incineration, industrial wastewater discharges, municipal wastewater discharges, and agriculture (Cordy et al., 2013;Chen *et al.*, 2012).

The three primary forms of mercury are organic compounds, inorganic salts, and metallic elements (Ghasemidehkordi et al., 2018). Each of these forms has a unique toxicity and bioavailability. These types of mercury are commonly found in water resources like lakes, rivers, and seas. They are absorbed by microorganisms and eventually undergo biomagnification, which seriously disrupts aquatic life. The main way that people are exposed to methylmercury is through eating this tainted aquatic animal (Jaishankar et al., 2014).

Mercury is used extensively in thermometers, barometers, pyrometers, hydrometers, mercury arc lamps, fluorescent lamps, and as a catalyst. It is also used in the pulp and

paper industry, as a component of batteries, and in dental preparations like amalgams (Jaishankar et al., 2014).

The neurotoxic chemical methylene-mercury leads to lipid peroxidation, mitochondrial (Alengebawy et al., 2021; Chai & Guo, 2023). damage, microtubule disintegration, and the build-up of neurotoxic substances such serotonin, glutamate, and aspartate (Patrick, 2002). An estimated 2,200 metric tonnes of mercury are released into the environment each year, according to Ferrara et al. (2000). The National Academy of Science and the Environmental Protection Agency estimate that 8 to 10% of American women suffer from exposure to mercury that could cause neurological abnormalities in any child.

Toxic mercury exposure has been linked to negative neurological and behavioural problems in animals. Rabbits subjected to 28.8 mg/m3 mercury vapour for 1–13 weeks revealed extensive cellular deterioration, brain necrosis, and vague pathological changes (Ashe et al., 1953). Although mercury may harm any organ and create problems in the kidneys, muscles, and nerves, its primary effects are still in the brain (Qin et al., 2023). It is possible for the intracellular calcium homeostasis and membrane potential to be disrupted.

According to Patrick (2002), mercury attaches to readily available thiols because of their high stability constants. Furthermore, it messes with transcription and translation, which eliminates the endoplasmic reticulum, makes ribosomes disappear, and activates natural killer cells. Temporary respiratory issues, asthma, and bronchitis can all be brought on by mercury fumes. Mercury binds to sulfhydryl and selenohydryl groups, which then

react with methyl mercury to harm tertiary and secondary protein structures and disturb cellular structure. Furthermore, the generation of free radicals is influenced by cell integrity (Jaishankar et al., 2014). Despite being stable and splitting into surrounding sulfhydryl-consisting ligands, the mercury sulfhydryl bond provides free sulfhydryl groups to promote metal mobility within the ligands, according to the heavy metal chelation theory (Bernhoft, 2011).

2.6 Human Health Assessment

Human health risk assessments are assessments of the potential health risks to individuals who may be exposed to environmental hazards (US EPA, 2022). Furthermore, the process that determines the kind and probability of detrimental health effects in people who may be exposed to chemicals in contaminated environmental media at any point in the future or right now is known as screening (Zhao et al., 2023). In quantifying a hazard and selecting a numerical figure to represent an actual threat, this method can be used for different situations. Scientific, engineering, and statistical fields produced these instruments ((Erickson, P. A. 1996; Hayes, 2023).

2.6.1 Dosage Response Assessment

In the dosage response phase, the extent of exposure and the likelihood that the relevant health effects would manifest are estimated (US EPA, 2022; Coulter, 2004).The link between the administration of an agent's dose and the emergence of a detrimental health consequence is explained by this procedure (Final, 1989; Mishra et al., 2019). In the case of the majority of toxic effects, such as those that are neurological, immunological, non-genotoxic carcinogenesis, reproductive, or developmental, it is widely accepted that there

exists a threshold (i.e., dose or concentration) below which harmful effects do not manifest. Other hazardous consequences are believed to be harmful at any exposure level. The non-threshold hypothesis is commonly employed in mutagenesis and genotoxic carcinogenesis (Zhao et al., 2023).

2.6.2 Exposure Assessment

The goal of hazard evaluation and dose-response assessment is to determine the kind and degree of chemical interaction experienced or predicted under different circumstances, and the exposure assessment is seen as a corresponding phase in those processes (Gündoğdu et al., 2020; USEPA, 2022). When computing the risk of exposure, consideration is given to the quantity of a toxic agent that enters the human body by any manner of vaporisation, oral, inhalational, and dermal exposure routes, as well as the total amount of the toxic agent present in the environment (USEPA, 2022). Exposure may be described as an ambient concentration if an assessment is restricted to a single exposure pathway (Nkansah et al., 2017). Thus, the exposure evaluation demands identifying a substance's emissions, routes, rates of movement, transformation, and degradation to infer the levels to which the human species and or the environmental domains (water, soil, and air) (Dartey & Gyamfi, 2024) would be exposed.

The application of the exposure assessment will depend on the numerical result, which could represent an estimate of the touch exposure's amount, intensities, rates, duration, or frequencies. During exposure evaluation, three key exposure channels are identified: cutaneous, oral, and breathing and vapourization when involving mercury investigation (Odukoya et al., 2018). Typically, risk evaluations based on dose-response relationships

result in an estimate of the dose. It is useful to note that the toxicological outcome of a given exposure is decided by the internal dose rather than the level of external exposure (Hayford et al., 2008). The expression "worst-case exposure" has typically referred to the highest level of exposure possible or the scenario in which all imaginable events would occur to raise exposure. Because it represents a hypothetical individual and an extreme set of circumstances that are generally not observed in an actual population, the exposure assessment is the "weakest link" in most risk assessments (USEPA, 2017). It is possible to obtain information about contamination by using biomarkers. However, it is untrue to presume that everyone experiences things that are the same or perhaps a normal quantity of contaminants because point sources are often the cause of pollution in hotspots (Mishra et al., 2019). By preserving the geographical distribution of soil contamination thresholds and receptors, the source-pathway receptor paradigm makes it feasible to estimate contaminant intake and, in turn, dangers more precisely (USEPA, 2011).

2.6.3 Risk-Characterization Management

At the end of the risk assessment process, researchers and risk managers receive risk characterization, which provides them with scientific data and rationale for the risk they wish to justify when making a decision USEPA (2017). All of the data from the hazard identification, dose-response, and exposure processes are quantitatively compared with dosages that are linked to possible health consequences to ascertain the real likelihood of danger to exposure populations (Dome et al., 2015). The term "risk management" refers to the actions required to determine if an associated risk should be avoided or minimized (Hayes, 2023). Regulatory, non-regulatory, economic, advisory, and technological risk management techniques or approaches can be broadly classified, but they are not

mutually exclusive (Zhang et al., 2023). The important decision-making elements, such as soil sample size, available resources, target-meeting expenses, and the scientific rigor of risk assessment and the consequent managerial judgments, vary substantially depending on the decision context (US EPA, 2022).

2.7 Chapter Summary

The increased potential toxic elements (PTE) pollution of Ghana's land/soil prompted (Country Environmental Analysis, 2020) this study, and this chapter evaluates health risk instances related to this issue. The chapter covered how mining-related solids (tailings) containing harmful heavy elements that cause cancer are becoming a significant problem in Ghana. It also covered how high concentrations of these toxic elements are released into the environment through surface water runoff, acid mine drainage, anthropogenic deposition, and tailings leaks, all of which have detrimental effects on the health of the local populations. To comprehend the genesis of element-causing diseases and susceptibility to human carcinogenesis, the chapter also covered heavy elements' chemical toxicity, exposure assessment, and potential mechanisms for their metabolic pathways (1997, 2006). The chapter also analyzed risk indices for human health, the environment, and pollution that are currently in use and were used to quantify the hazards and pollution this study looked at. The integrated approach was determined to be the most effective strategy for the computation when the chapter finally looked at the geochemical baseline estimation techniques.

CHAPTER THREE

MATERIAL AND METHODS

3.1 Study Area

Atwima Mponua District, the study area, is located in the southwestern part of the Ashanti Region. This District is one of the 261 Metropolitan, Municipal, and District Assemblies (MMDAs) in Ghana, and forms part of the 43 MMDAs in the Ashanti Region with Nyinahin as its administrative capital. The district has 310 communities, which are grouped into 11 Area Councils, and divided into 38 Electoral Areas (Atwima Mponua DA, 2019). The district occupies 1,883.2 km2 of land and is located between latitudes 6º32'N and 6º75'N and longitudes 2º00'W and 2º32'W (Atwima Mponua DA, 2019). The district is bounded to the south by the Amansie West District, to the east by the Bibiani Anwhiaso Bekwai Municipality in the Western North Region, to the north by Ahafo Ano South West, and to the west by Atwima Nwabiagya South Municipality. According to the 2021 Population and Housing Census, there are 155,254 people living in the Atwima Mponua District, with 80,235 men and 75,019 women. The district's economy is thought to be primarily based on agriculture

(ATWIMA MPONUA DISTRICT, 2014-2017). A map of the study area that displays the sampling locations in the Atwima Mponua District is shown in Figure 1.

The district has undulating topography dissected by plains and slopes with an average height of 70 m above sea level. The high grounds are parts of the Atwima-Atakpame mountains range that lies to the northwest of the district. It is drained mainly by the Tano and Offin Rivers. These rivers flow continually throughout the year and can therefore be

used for both domestic and agricultural purposes. The vegetation is basically of the semi-deciduous type. The flora and fauna are diverse and composed of different species of both economic and ornamental trees with varying heights, game, and wildlife. There is a vast economic potential for timber-based value-adding industries. The soils in the district are generally suitable for agriculture. They are classified into two usage characteristics: moderately suitable and marginally suitable soils. These soils are deep and can support a wide range of cash, food, and tree crops. It is underlain by the Birimain and Tarkwaian rocks, which are rich in minerals such as gold, bauxite, and Gold-bearing rocks. Bauxite is found at Nyinahin, however, it remains unexploited (ATWIMA MPONUA DISTRICT, (2014-2017). It can be expected that exploitation of the minerals in the district will greatly energize the development of the district through job creation and improved household incomes of the population in the district.

The expected coverage of the road network is 452.4 km. The district's roadways are mostly unpaved, dusty, and uneven, with the exception of 60.8 km of First-Class Road that connects the capital to the Kumasi-Sunyani Road at Abuakwa from Bibiani and beyond. Like most Ghanaian rural districts, the Atwima Mponua District is mostly an agrarian one. Agriculture employs the majority of people, with manufacturing, services, and commerce coming in second and third. Manufacturing activities in the district are light manufacturing, lumbering, and agro-processing. The industries are practised on a small scale and are next in importance to agriculture, commerce, and trading. The small and medium-scale enterprises are in the areas of wood-based industries, mining, metal works, block moulding, gari production, akpeteshie distillery, corn milling, and others.

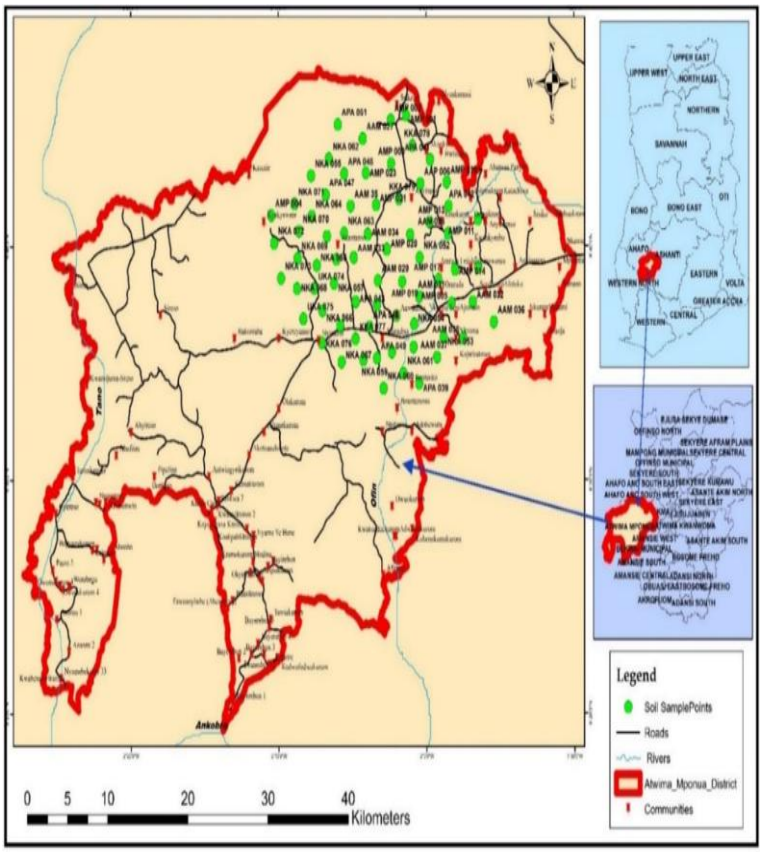

Figure 3.1. Map of the study area at Atwima Mponua District with Green colour indicating the exact location of the sampling points

3.2 Soil Sampling

A clean, dry plastic shovel was used to gather about 500 g of soil at a surface soil level of 0 to 15 cm. This gives a better assessment of the risk to human health because it presumes that this is the area that people are most likely to come into contact with during daily activities. Seventy-eight (78) soil samples using a transect method, with samples taken at 5 m intervals to capture spatial variation. Additionally, a 100 × 100 m grid was

used for mapping and sampling at coordinate intersections, where sampling was not possible due to obstructions such as tarred roads, rivers, or houses, sampling locations were adjusted by moving 2 m to either the left or right of similar equidistance point, using a clean dry plastic hand trowel, soil samples were collected from each sampling location following the removal of plants and superficial debris, from thirty (30) distinct settlements in the Atwima Mponua District that are representative of the area.

A composite sample was created by randomly selecting four (4) replicate samples around 5 m away from the first sampling spot and thoroughly mixing them; one gram of matter of the homogenous mixture was then placed in plastic bags. A Global Positioning System (GPS) was used to appropriately mark, code, and identify each of the uniform samples that were gathered based on their sampling positions. The coded samples were taken to the laboratory for further processing.

3.3 Soil Preparation

The soil samples were air-dried under a fume chamber, and homogenised by grinding using a mortar and pestle before passing them through a screen with a mesh size of 250 µm using USA Standard Testing Sieve ASTM E11 to remove any leftover plant pieces, stones, or other items. To avoid cross-contamination, the mortar, pestle, and sieves were cleaned with fresh tissue paper after each grinding and sieving.

3.4 Instrumental Analysis

3.4.1 Field Portable X-ray Fluorescence (FP-XRF) Spectrometer

The elements' As, Cd, Co, Cr, Cu, Fe, Mn, Ni, Pb, Ti, V, and Zn Concentrations were determined with a Thermo Scientific Niton XL3t GOLDD + field portable X-ray fluorescence (FP-XRF) spectrometer. The sample holder covered with a Mylar film at one end was filled two-thirds full with the soil sample. The sample holder was then placed in the XRF shroud and scanned for 180 s to obtain the desired result. All the samples were treated in the same manner. All the XRF sample analysis was done in triplicate. The equipment was calibrated with reference material (Mackey et al., 2009) and the recovery rates in the range of 90 and 116% were sufficient for analysis.

Plate 3.1: Niton XL3t GOLDD + field portable X-ray fluorescence (FP-XRF) spectrometer

3.4.2 Mercury Analysis

PYRO-915+ attachment and RA 915 M Zeeman Mercury Analyzer (Lumex, Ohio, USA) were employed to determine the mercury concentrations in soil samples of the investigated communities (Rweyemamu et al., 2020; Asamoah et al., 2023

Plate 3.2: PYRO-915^{+} and RA 915 M, Mercury Analyzer (SHEATHE Lab, KNUST)

3.4.3 Quality Assurance

To ensure the validity, reliability, and accuracy of the data in this study, several quality assurance and control measures were employed. Soil samples were carefully handled in the laboratory and on the sampling site to avoid contamination. The samples were stored in polyethylene zip-lock bags that were permanently identified and tightly sealed to avoid contamination, muddling, and mixing. All sampling and sieving equipment, such as the shovel, plastic container, brush, test sieve, mortar, and pestle, were meticulously cleaned to reduce the possibility of cross-contamination. A Niton XL3t field portable X-ray fluorescence spectrometer was used to screen samples for potentially hazardous elements following US Environmental Protection Agency Method 6200 for metal analysis. Every day before the soil was analyzed, a NIST 2710a reference material was run, and the XRF system was checked. This consistently produced a recovery of > 75 ± 5%. An acceptable average relative percentage difference was produced by the repeatability test (21% for As, 11% for Cu, 9.2% for Ni, 13% for Pb, and 7.7% for Zn)(Asamoah et al., 2023). The

average of the readings was calculated after each sample analysis was completed in triplicate.

3.4.4 Determination of Soil pH and Electroconductivity

Soil samples were dissolved in measured distilled water at 1:2.5 and 1:5 (w/v), soil-deionized water suspension for pH and electrical conductivity (EC) measurements, respectively. This was performed by weighing 20 g air-dried soil into a beaker, then 40 mL of distilled water was added and the beakers were manually shaken and thoroughly stirred using an electronic stirrer Hn201Q for 10-minute intervals for 1 hour to allow soluble salts to dissolve and ionic exchange to reach equilibrium before estimating pH. Soil EC was measured using a calibrated Hanna EC meter H28116731 DiSt-6, and pH was measured using a Hach H550 Rugged Pocket pH meter. Soil particle spatial distribution was estimated by the use of both manual and mechanical sieving. The manual analysis and mechanical sieving were carried out at the chemistry laboratory of Akenten Appiah-Menka University of Skills Training and Entrepreneurial Development, Mampong campus. Thus, in each technique, soil aggregates were broken manually before sieving. The results were estimated to find the percentage aggregates of textural fractions in the soil. First, the pH meter was calibrated by submerging the pH electrode in a buffer solution with a known pH of 4 and calibrating the apparatus to read the buffer's solution. Following a cleaning with distilled water, the standard electrode was submerged in a second buffer solution (pH = 9), and the pH of the buffer was measured using the instrument. Instrument values were first normalized using this process. After that, the pH meter's electrode was dipped in a water sample and rinsed three times using some of the samples that were going to be analyzed. The pH meter numbers were meant to remain

steady, therefore this was done. After the device calibration process, the multifunctional HI-9835 meter was utilized to quantify electrical conductivity and total dissolved solids (TDS). Before inserting the probe into a sample solution, it was cleaned with deionized water. After completely submerging the probe into the sleeve apertures, any trapped air bubbles were repeatedly tapped out.

Plate 3.3. Hanna H28116731 DiSt-6 EC meter: Hach H550 Rugged Poket pH meter

The loss-on-ignition method was used to determine the total organic carbon in the soil sample (Darko et al., 2019). Briefly, a 1-gram aliquot of soil sample was directly weighed into a crucible and heated at 105 ^{o}C for 2 hours. After cooling to room temperature in a desiccator, the soil samples were placed in a pre-heated thermocline muffle furnace at

550 ^{o}C for 8 hours. The samples were removed from the furnace, cooled to room temperature (overnight) in a desiccator, and re-weighed. Organic matter content is determined by calculating the difference between initial and final weights. The analyses were done in triplicates.

3.5 Soil Contamination Assessment

The degree of contamination with potentially toxic elements can be measured by comparing the collected data to background reference data, using pollution indices, and the potential ecological risk index (PERI). In this study, contamination was assessed through the use of pollution indices and the comparison of site-specific data to background reference data. To establish a reliable assessment of the site's quality, the levels of potentially toxic substances in the soil samples were contrasted with their corresponding international standards (VROM, 2000; CCME, 2007) because of their consistent usefulness in other conducted research studies in Ghana and the world at large.

3.6 Pollution Indices

The study evaluated the pollution status of the topsoil (0-15 cm) of the soil samples contaminated with potential toxic elements (PTEs) using pollution indices: contamination factor (CF), geo-accumulation index (Igeo), enrichment factor (EF), and potentially ecological risk index (PERI) to help predict the potential ecological risk of the study area.

3.6.1 Geo-accumulation index (Igeo)

The geo-accumulation index was proposed by Muller, (1979) to assess the concentration of potentially toxic elements that have accumulated in soil over the baseline

concentration since preindustrial times. Unlike other methods of pollution evaluation, Igeo considers the natural diagenetic process, making its results more realistic ((Thiombane et al., 2023).

$$\text{Geo-accumulation index } I_{geo} = \log_2\left(\frac{C_n}{1.5 \times B_n}\right) \quad \text{Eqn. 1}$$

Cn is the observed element's mean concentration in the soil samples, and *Bn* is the geochemical baseline value concentration. The background matrix is adjusted for any changes caused by the anthropogenic and lithogenic effects using a factor of 1.5 (Asamoah et al., 2023; Konadu et al., 2023). I_{geo} is classified into seven classes (Baah et al., 2023); Tawabini et al., 2023).

Table 3.1: Classes of I_{geo} Values and Description

I_{geo} Class	I_{geo} Value	Soil Quality
0	≤0	Uncontaminated
1	0-1	Uncontaminated to moderately contaminated
2	1-2	Moderately contaminated
3	2-3	Moderately to heavily contaminated
4	3-4	Heavily contaminated
5	4-5	Heavily to extremely contaminated
6	≥5	Extremely contaminated

(Asamoah et al., 2023; Chonokhuu et al., 2019; Kanson, 1980)

3.6.2 Enrichment Factor

The enrichment Factor described in equation four (Eqn. 2) was used to assess the levels of PTE pollution from anthropogenic sources as well as differentiate between anthropogenic and naturally occurring sources (Konadu et al., 2023; Mensah et al., 2020)

Enrichment factor (ErF) = $\frac{M_c \times F_{er}}{M_r \times F_{ec}}$ Eqn. 2

Enrichment factor (ErF); M_c and F_{ec} are the sampled PTE and iron concentrations in the study area, respectively, while M_r and F_{er} are the PTE and iron concentrations in the soil samples. (Asamoah et al., 2021; Nkansah, Darko, Dodd, Opoku, Bentum Essuman, et al., 2017). Erf recognized that the contents of elements of Fe and Al occur in a natural medium and are primarily geogenic, hence Fe was employed as the normalization element in computing the enrichment because it has a slightly greater concentration in the natural environment (Asamoah et al., 2023; Mensah et al., 2021).

ErF > 1 indicates enriched PTE concentrations, likely anthropogenic, while ErF < 1 indicates geogenic sources (Konadu et al., 2023). ErF characterized anthropogenic contaminants as diplayed in appendix 4; low (ErF = 1.5 – 3), moderate (ErF = 3 – 5), severe (ErF = 5 – 10), or very severe (ErF > 10).

3.6.3 Contamination factor

The contamination factor measures the amount of anthropogenic input in elemental pollution (Dartey & Gyamfi, 2024). It is commonly used to assess the overall PTE contamination of soil. The contamination factor (CF) is the ratio of the concentration of PTE in the soil to the background concentration, mathematically shown in Equation 3.

Contamination factor (CF) = Mx/Mr Eqn. 3

Where Mx and Mr are the mean concentrations of the metal in the soil samples and background reference value, respectively (Dartey & Gyamfi, 2024; Konadu et al., 2023) The designation of the CF classes is indicated by an index range of CF < 1= low contamination; 1 to 3 = moderate contamination; 3 to 6 = considerable contamination, and > 6 = very high contamination (Asamoah et al., 2021), as shown in Appendix 4.

3.6.4 Potential Ecological Risk Assessment

The potential ecological risk (PER) and index (PERI), which are based on the contamination factor of PTEs (CF) and the environment's response to the contamination (Trf), were used to measure the risk to the ecological environment. The PERI was calculated as the sum of individual potential ecological risk factors (PER) as shown in Equations 4 and 5.

PER = Trf x CF Eqn. 4

PERI = $\sum_i^n Trf \times CF$ Eqn. 5

The toxic response factors (Trf) of the PTEs are Zn = 1, Mn = 1, Cr = 2, V = 2, Pb = 5, Cu = 5, Ni = 6, As = 10, Cd = 30, and Hg = 40 (Konadu et al., 2023). Table 3.2 classifies ecological danger according to its level.

Table 3.2. The different categories of potential ecological risk are in degrees.

Degree of ecological risk	Classification
PER< 40	low risk
40 ≤ PER < 80	moderate risk
80 ≤ PER < 160	considerable risk
160 ≤ PER < 320	high risk
PER ≥ 320	very high risk
PERI ≤ 150	Low
150 ≤ PERI < 300	Moderate
300 ≤ PERI < 600	Considerable
600 ≤ PERI	Very high

(Hakanson, 1980; Darko et al., 2017; Dartey & Gyamfi, 2024)

3.7 Correlation Analysis

Correlation analysis is an empirical method used in research to investigate the degree of linear relationship between two variables and determine their linkage (Braeken & Van Assen, 2017). According to Liu et al. (2021), whereas a low correlation denotes a weak relationship between the two variables, a high correlation indicates a strong one. A positive correlation exists when there is a rise in one variable leads to an increase in the other (Zhu et al., 2022). A negative correlation, on the other hand, reveals that while one of the factors increases, the other lowers, and vice versa (Suryawanshi et al., 2016). The correlation coefficient, represented by the symbol r and usually a value with units falling between 1 and -1, is the unit of measurement used for analyzing the intensity of the linear relationship between the variables involved in correlational data analysis (Braeken & Van Assen, 2017). Two variables may correlate positively, negatively, or not at all. Any score between + 0.5 and +1 denotes a very high positive correlation, or the notion that they both rise at the same time (Zhu et al., 2022). A substantial negative correlation is

indicated by any number between -0.5 and -1, which means that when one measure rises, the other declines correspondingly (Suryawanshi et al., 2016). A score of 0 indicates that there is no association or correlation between the two variables (Braeken & Van Assen, 2017).

3.8 Source Apportionment

3.8.1 Positive Matrix Factorization (PMF) Model

The US Environmental Protection Agency (USEPA) recommends positive matrix factorization (EPA PMF version 5.0), as an effective multivariate receptor model for apportioning pollution sources (Jiang et al. 2017). Toxic elements can enter soils from several sources, and their concentrations are cumulative. The PMF model effectively computed source profile and source contribution using reliable factorization techniques and decreased multi-dimensional data by extracting hidden characteristics in soil for analysis (Alengebawy et al., 2021; Huston et al., 2012). Brown, Paatero, and Tapper (year) present an in-depth mathematical explanation of positive matrix factorization.

$$e_{ij} = \sum_{i=1}^{n} g_{ik} + f_{jk} + x_{ij}$$ Eqn. 15 (Brown et al., 2015)

In this equation, **eij** represents the concentration source's profile (element content j in soil sample i), p indicates the number of factors, gik represents the factor's contribution to soil sample i, fjk represents the element content profile j in factor k, and xij defines the residuals of each element species. Another PMF model can be used to examine each factor's contribution and source profiles. The objective function (Q) is expressed as: (Qin et al., 2021)

$$Q = \Sigma_{i=1}^{n} \Sigma_{j=1}^{m} \left(\frac{x_{ij}}{u_{ij}}\right)^2$$ Eqn.16

Where n is the number of samples, m is the number of PTEs determined, and u_{ij} Is the uncertainty of PTM j in soil sample i Uncertainty can be measured using element content eij, technique detection limit, and relative standard deviation (σ). To assess uncertainty (u_{ij}), use a fixed fraction of the MDL. When the PTM concentration exceeds MDL, u_{ij}. This can be calculated as:

$$u_{ij} = \sqrt{[Error\ Fraction\ (ErF) \times Concentration\ (C)]^2 + (0.5 \times MDL)^2}$$

Eqn. 17

Or

$$u_{ij} = \sqrt{(\sigma \times C)^2 + (MDL)^2}$$ Eqn. 18

(Brown et al., 2015; EPA Epa Exposure Research Lab.2021)

When the element is less than or equal to the method detection limit (MDL), u_{ij}. This can be calculated as:

$$u_{ij} = \frac{5}{6} \times MDL$$ Eqn. 19 (Epa & Exposure Research Lab., 2021)

Where **σ** is the relative standard deviation and C is the concentration of the chemical element. In the present study, positive matrix factorization 5.0 software (USEPA 2014) was employed to apportion concentrations and contributions of different sources to PTE in the soil of Atwima Mponua District, Ghana.

The B% species and concentrations of elements loaded from different source profiles of the base (BS-DISP) run, bootstrap (BS) run, and base model displacement (DISP). The base run errors were within the interquartile range (25th-75th) of the BS, DISP, and BS-

DISP runs (Fig. 3A), showing that PMF base run fitting errors were acceptable. The high determination coefficient and tolerable error indicated a sufficient number of sources and a robust PMF model (Paatero et al., 2003; Qin et al., 2021). G: The specific source contribution of each element pollution. E: Total contribution from each source category for accuracy confirmation. The PMF model was also employed to establish the lowest Q value where the residue lay between -1 and + 1 for five to seven (5-7) factors were assessed, and the system was set to run 20 times under different conditions for the best solution to be obtained.

3.8.2 Principal Component Analysis (PCA)

PCA is a data reduction technique that is used to decrease the number of variables to a few uncorrelated components (Song et al., 2019). It aims to justify most of the data's variability. The principal component scores and loadings are the correlations between the data points and the principal components, were deployed to effectively utilize principal component analysis (PCA) to categorize individuals and groups of variables (Huang et al., 2022; Asamoah et al., 2023) When employing bilinear modeling techniques, the output of PCA software is often a graph known as "scores" (equal to the variables), which condenses the statistical data contained by many variables onto a small number of underlying variables (Jolliffe et al., 2016). Every sample's model component has a score. According to Rabin et al. (2023), sample trends, clusters, similarities, and discrepancies can be found using the scores, which show the samples' placements along each model component. Bilinear modelling approaches are used to estimate a "loading," one of the supplementary graphs produced by PCA. This is a process where data from several variables is condensed into a limited number of components. Every variable is loaded in

tandem with every segment of the model (Ghasemidehkordi et al., 2018; Ozturk et al., 2022). Each variable's level of accounting for each component of the model is shown by the loadings. They can be applied to identify the relative contributions of each variable to the significant variance in the data as well as to interpret the relationships between variables. According to Jolliffe et al. (2016), they also aid in determining the importance of each model component. An abundance of computational techniques has been developed for PCA. According to Huang et al. (2022), some computation approaches find all the components at once, whereas others find the most important component first, then the next component, and so on.

3.9 Human Health Risk Assessment

Human health risk assessment helps determine the risk of contaminant exposure in workplaces and the community, protecting workers as well as inhabitants of the community. The effects of pollution or heavy metals on humans and the environment depend on their chemical characteristics, particle sizes, and exposure time (Konadu et al., 2023). Heavy metals exposure can occur through direct ingestion (Bing), inhalation (Binh), dermal absorption or contact (Bderm), and vapourization (Bvap) in the case of mercury, (Konadu et al., 2023). The average dose exposure pathways of PTEs have their parameters defined in Table 3.3.

Table 3.3 Exposure factors and the reference value of the parameters

Factor	Units	Definition	Value	
	mg/cm^2 /day	Dose	B_{dern}, B_{ing}, and B_{inh}	
Notations	mg/kg	Concentration	concentration of PTE in (exposure point concentration)	
			Children	Adults
C_{soil}	mg/kg	Concentration of elements in the soil sample		
SA	cm^2	Exposure skin area	4,200	13,110
ABS	no unit	Dermal absorption factor	0.1	0.1
SL	mg/cm^2 /day	Exposure adherence factor	0.2	0.07
Ingf	mg/day	Ingestion rate	400	100
Inhf	mg/day	Inhalation rate	10	10.4
BW	kg	Body weight	15	70
CF	mg/kg	Convention factor	1.00E06	10^{-6}
ED	year	Exposure duration	6	30
VF	mg/kg	Volatilization factor	8,028.297	8,028.297
EF	days/year	Exposure frequency	365 (180)	365 (180)
PEF	mg/kg	Particle emission factor	725,000,000	322,000,000
$AT_{non\text{-}can}$	days	Average time for non-carcinogens	2190	10,950
AT_{car}	days	Average time	15×365	70×365

The dose is contracted through inhalation (Binh), ingestion (Bing) of substrate particles, and absorption through dermal contact with substrate particles (Bderm), and vaporisation (Bvap).

The dose intake through each pathway: ingestion (Bing), inhalation (Binh), dermal absorption or contact (Bderm), and vapourisation (Bvap) is calculated using Eqns. 6, 7, 8, and 9, respectively (Asamoah et al., 2023; Odukoya et al., 2018).

$$Binh = C_{soil} \times \frac{Inhf \times EF \times ED}{PER \times BW \times AT} \times 10^{-6} \quad \text{Eqn. 6}$$

$$Bing = C_{soil} \times \frac{Ingf \times EF \times ED}{BW \times AT} \times 10^{-6} \quad \text{Eqn. 7}$$

$$Bderm = C_{soil} \times \frac{SL \times SA \times ABS \times EF \times ED}{BW \times AT} \times 10^{-6} \quad \text{Eqn. 8}$$

$$Bvap = C_{soil} \times \frac{Inhf \times EF \times \times ED}{VF \times BW \times AT} \quad \text{Eqn. 9}$$

C_{soil} is the PTE concentration in topsoil; BW is the average body weight (kg); SA is the exposure skin area (cm^2); PEF is the particle emission factor (mg/kg); ABS is the dimension dermal absorption factor; SL is the skin adherence factor (mg/cm/d); AT is the average time (d); Erf is the exposure frequency (d/a); ED is the exposure duration (a); and Cf is the conversion factor (10^{-6}, mg/kg) ED × 365 days for non-carcinogenic risk and 72 × 365 days for carcinogenic risk; *Binh, Bing, Bderm, and Bvap* are the rates of inhalation, ingestion, dermal contact and vapourization, respectively.

Table 3.4. Reference doses of the PTEs for various pathways (Aguilera et al., 2021; Fabiana Meijon Fadul, 2019; Nkansah, Darko, Dodd, Opoku, Essuman, et al., 2017)

PTEs	Bing RfD	Bderm RfD	Binh RfD	SF
As	3.00E-04	1.23E-04	3.01E-04	1.51E+00
Cd	1.00E-03	1.00E-05	1.00E-03	6.30E+00
Co	2.00E-02	1.60E-02	5.71E-06	
Cr	3.00E-03	6.00E-05	2.86E-05	4.20E+01
Cu	4.00E-02	1.20E-02	4.02E-02	
Fe	8.40E+00	7.00E-02	2.20E-04	
Hg	3.00E-04	2.10E-05	8.57E-05	
Mn	4.60E-02	1.85E-03	1.43E-05	
Ni	2.00E-02	5.40E-03	2.06E-02	
Pb	3.50E-03	5.25E-04	3.52E-03	4.47E+00
V	7.00E-03	7.00E-05	7.00E-03	
Zn	3.00E-01	6.00E-02	3.00E-01	

Bing: ingestion, Binh: inhalation, Bderm: dermal absorption or contact, RfD: reference doses, E: exponential, SF: slope factor.

Equation 10 is used to calculate the non-carcinogenic or non-cancer risk of exposure.

$$HQ = \frac{SF}{RfD} \qquad \text{Eqn. 10}$$

In this equation, HQ represents the hazard quotient for a specific route of exposure, SF represents the dose taken in, and RfD represents the reference dose for a particular element through an identifiable route.

3.9.1 Hazard Index (HI), Total Hazard Quotient (THI)

The Hazard Index (HI) is the total of all the HQ for each pathway equation (Eqn. 6 – 9) (Dartey & Gyamfi, 2024), the total hazard index (THI) is the sum of the HI of the potentially toxic elements under assessment (Darko et al., 2022; Dartey & Gyamfi, 2024). HI < 1 or HQ < 1 indicates no significant risk of non-carcinogenic hazard risk while HI > 1 or HQ > 1 implies the likelihood of non-carcinogenic hazard risk present respectively which is enhanced with increasing HI values (USEPA, 2001, Carla et al., 2014). The hazard quotient (HI) and total hazard quotient (THI) are calculated by the utilization of the equations (Eqn. 11, 12) (Darko et al., 2022; Dartey & Gyamfi, 2024; Odukoya et al., 2018).

$$HI = \sum_i^0 (HQi) \qquad \text{Eqn. 11}$$

$$THI = \sum_i^0 (HQi) = HIj \qquad \text{Eqn. 12}$$

The hazard index is well recognized as a helpful tool for assessing health hazards from pollutants. An index below one (THQ < 1) indicates minimal or negligible non-cancer influence and no adverse effects on health. A threshold above one (THQ > 1) raises

concern about potential health consequences (Dartey & Gyamfi, 2024a; Konadu et al., 2023).

3.9.2 Carcinogenic Risk Assessment

Carcinogenic risk is the probability of an individual developing any type of cancer over a lifetime, as a result of exposure to carcinogens. The total carcinogenic risk (TCR) is the sum of the carcinogenic risk (CR) of PTEs. Eqn. 13 and 14 were used to compute the CR and TCR, respectively. The cancer slope factor (mg/(kg d) is represented by CSF (Dartey & Gyamfi, 2024). The study took into account As, Cd, Cr, and Pb due to their potential carcinogenicity. Carcinogenic risk is negligible if CR is less than 1 × 10-6 (Dartey & Gyamfi, 2024; Konadu et al., 2023). Table 3.5. displays the cancer slope factor (CSF) and reference dose values (RfD).

CR = RfD x CSF Eqn. 13

TCR = $\sum_{j=1}^{n} CRj$ Eqn. 14

Table 3.5. Values for Cancer Slope Factor (CSF) and Reference Dose Values (RfD) in mg $kg^{-1}d^{-1}$ (Kamunda et al., 2016)

Elements	CSFing	CSFinh	CSFderm
As	1.5	1.50E+01	3.66E+00
Cd	NA	6.3	2.00E+01
Cr	5.00E-01	4.02	2.00E+01
Pb	8.50E-03	4.20E-02	NA

(Kamunda et al., 2016), (Konadu et al., 2023; Rinklebe et al., 2019)

3.10 Statistical Analyses

Statistical analyses were accomplished by employing JASP, MINITAB, and EPA PMF 5.04 software. Five basic statistical methods – Descriptive Statistics, Correlation, Regression analysis, Principal Component Analysis (PCA), and Positive Metrics Factorization (PMF)- were used to estimate the source profile and source contribution of PTEs in the area of study. The dataset base is continuous; thus, Pearson's correlation analysis was used to assess the concentrations. The geographic information system (GIS) technologies were employed and validated.

CHAPTER FOUR

RESULTS AND DISCUSSIONS

4.1 Heavy Elements Concentrations in Soil

This study compared its results to values from the control location for PTEs in soil set by the Canadian Council of Ministers of the Environment (CCME 2007), Dutch International Values (VROM 2000), and South Africa Guidelines – Dept. of Environment Affairs (DEA), 2010. This is because Ghana does not currently have any soil quality guidelines. The statistical overview of the analysis is shown in Table 2.

Table 4.1. Descriptive Characterization, International Standards for PTEs in Soil

PTEs	Mean	Variance	Minimum	Median	Maximum	Skewness	Kurtosis	VROM 2000	CCME 2007	DEA 2010
As	9.095	53.443	3.18	6.81	42.79	2.57	7.62	29	12	5.8
Cd	204.22	2385.86	6.42	213.67	253.44	-3.34	11.34	0.8	22	7.5
Co	121.16	2839.18	50.56	109.06	279.61	1.3	1.33	9	300	300
Cr	2.9	109.12	0.39	0.49	53.5	4.24	16.69	100	130	6.5
Cu	15.473	10.406	12.41	14.61	32.43	2.93	10.95	36	91	16
Fe	21725	2.60E+08	4826	16499	90763	2.13	5.34	N/A	N/A	N/A
Hg	6.762	0.895	4.54	6.635	9.81	0.69	1.74	0.3	50	N/A
Mn	361.8	226481	34.6	285.6	4313.2	7.69	63.74	N/A	N/A	N/A
Ni	26.303	12.038	16.78	25.985	36.3	0.22	2.06	35	50	91
Pb	4.992	3.541	3.14	4.73	18.32	5.72	36.92	85	600	20
Ti	264	878395	18	46	4969	4.22	16.57	N/A	N/A	N/A
V	4.47	210.42	0.88	1.21	88.24	4.6	21.08	42	N/A	N/A
Zn	39.56	270.81	13.98	34.45	102.28	1.58	3.13	140	360	240

Canadian Council of Ministers of the Environment (CCME 2007): Dutch International Values (VROM 2000): and South Africa Guidelines – Dept. of Environment Affairs (DEA), 2010: N/A means not available

4.1.2. Multivariate, Correlation, and Statistical Analyses

The study also used the Anderson-Darling and Shapiro-Wilk tests to confirm the data's normality (Najmeddin et al., 2017). The results indicate that all PTEs (except Hg) are normally distributed in the soil samples (significance level < 0.001). Additionally, the results based on normalized skewness and kurtosis suggested that the nature of these data sets is continuously distributed (Table 4.1). Spearman's correlation coefficients and principal component analysis were used to discover the association between PTEs in soil samples and their likely sources of pollution. Factor analysis was employed in the surface soil data set to derive underlying components that describe the covariance among variables.

This analysis decreases multi-dimensional data by extracting hidden characteristics (Gallego et al. 2002; Keshavarzi et al. 2012) and aids in the identification of groups with common properties. Kaiser-Meyer-Olkin (KMO) and Bartlett's tests were used to assess the possibility of running factor analysis on the data set (Ho 2013). The KMO (0.567) and Bartlett's test ($p < 0.001$) indicated that Principal Component Analysis (PCA) was appropriate for this data set. The Kruskal-Wallis (H test) is a nonparametric rank-based test that can be used to assess if there are statistically significant differences in a continuous or ordinal dependent variable across three or more independent variable groups (Najmeddin et al., 2017).

The mean levels of Co, Hg, and As are higher than their VROM and DEA corresponding background values (BV) of soil. The mean concentration of other heavy metals in each sample was below the permissible scope. All the heavy metals in the soil of the study

region, according to the results, compared to either one or all of the corresponding standards by CCME (2007), VROM or DEA, mean background value in soil, except for Mn, V, and Ti, which have no or unavailable reference values for justification. The average accumulation rate (Cmean/BV) for Co, Pb, As, Hg, Zn, Cu, Ni, Co, and Cr were 9.2827, 0.0083, 0.7579, 0.061, 0.1099, .01700, 0.5261, 0.4039 and 0.0223, respectively. This suggests that the study area has been mildly contaminated by lithogenic activities, except for Cd, which can be attributed to the anthropogenic source. Anderson-Darling Normality test predicts the ecological spread of heavy metals in the mining sites ($p < 0.005$), indicating a highly statistically significant variance. The high coefficients of variation (CV = standard deviation/mean) and standard deviation for certain PTEs indicate notable heterogeneity in their spatial distribution (Jiang et al., 2017; Najmeddin et al., 2017). When the CV is greater than 0.3, the characteristics are regarded statistically as highly variable and widely distributed (Mashal et al. 2015). As a result, the concentrations of Cd, Pb, As, Hg, Zn, Cu, Ni, Co, Fe, Mn, Cr, V, and Ti varied significantly across the soil samples (Table 2). Both natural and man-made factors could be the cause of this heterogeneity.

Compared to typical pollution sites like mines, smelters, and electronic waste dumpsite soils, cadmium concentrations in this study area are significantly higher and are on the same order of magnitude as the average level reported by other studies (Jiang et al., 2017; Konadu et al., 2023; Opoku et al., 2020). All elements (apart from Hg) have positive skewness values toward the higher concentrations, indicating that their mean concentrations are greater than their median concentrations. Except for Zn, Ni, and Hg, all PTEs have kurtosis values greater than 3, indicating that the distributions of these

elements' concentrations in the samples are steeper than usual. Skewness and kurtosis values for regular soil metals (Mn, Pb, V, Cr, Ti, and Cd) tend to be higher than those for other elements, indicating the presence of heavily contaminated areas.

4.2 Physicochemical Parameters of Soil

Table 4.2 Physicochemical parameters of PTEs in Soil

	pH	OTC	EC (µs/cm)	One Sample T-Test			
Mean	5.96	21.71	68.83		T	df	P
Min	4.91	13.18	12.495	AVG	12.08	76	0.001
Max	8.24	33.37	275.9				
Median	5.93	21.37	57.94				
Std.dev	0.69	5.53	49.67				
Kutosis	0.02	0.36	5.53				

EC: Electrical Conductivity, TOC: Total Organic Carbon: 1-sample T-test

4.2.1. Soil pH

The pH of the soil plays a crucial role in monitoring the transfer and element concentration in the soil (Ali et al., 2019; Ashaiekh et al., 2019; (Konadu et al., 2023). The mean soil pH in the Atwima Mponua District was 5.97, which indicated weak acidic soil characteristics. In addition, the soil samples from the sites recorded a minimum value of 4.91 and a maximum value of 8.25, indicating that soil pH in the examined area may have a characteristic between weakly acidic medium and weakly alkaline medium. This trend is in line with soil properties found in the mining communities (Asamoah et al., 2023). The pH of the soil may be one of the primary factors influencing the composition of the solution since it regulates the mobility of PTEs, according to Kulikowska and Klimiuk (2008). This characteristic may be traced to the nitric acid and carbonic acid production as a result of Au-Ag mining, fertilizer discharge, pesticides, and trash dumping (Kormoker et al., 2019; Pobi et al., 2020) in the area. The estimated mean pH

is statistically significant (p-value = 0.001, to $p < 0.05$). Since pH regulates the accessibility of soil nutrients and other chemical components or elements to plants, it is an influential component in all stabilization processes (Calli et al., 2005). Therefore, the soil sample pH may influence the rate of PTE migration and retention in soils. PTEs exhibit better retention and reduced solubility at higher soil pH, possibly due to their capacity to form complexes at higher pH (Asamoah et al., 2023; Obiri et al., 2016). Thus, PTE complexes are expected to be available for uptake by plants and other organisms present (Odom et al., 2021; Opoku et al., 2020).

4.2.2 Electrical Conductivity

The concentration of element ions in the soil is indicated by the soil's electrical conductivity. The higher electrical conductivity predicts a high concentration of dissolved salts in the soil, which is linked to a higher mobility of free element ions (Yuan et al., 2021; (Asamoah et al., 2023). The observed mean Electrical Conductivity from soil samples in the Atwima Mponua District communities is 69.44 with a minimum value of 12.50 and maximum value of 275.9, all in µS/cm. With a p-value of 0.001 ($p < 0.005$), there was a highly significant difference in the EC values. The mean readings for the study communities are much below the CCME soil quality recommendation of 2,000 µS/cm (CCME, 2007), suggesting that the surface soils have low amounts of inorganic ions (Acheampong et al., 2018; Asamoah et al., 2023). Soil solution conductivity is mostly caused by dissolved ions, particularly salts, which have an impact on electrical conductivity. Soils affected by anthropogenic activity typically exhibit significant levels of electrical conductivity.

4.2.3 Total Organic Carbon

Total organic carbon (TOC) levels at the mining site ranged from 13.18 to 33.37, with a mean of 21.78. The one-sample T-test results ($p = 0.001$) show normal distribution, and the calculated mean is statistically significant. The total organic carbon content values ranging from 2.20 to 8.90% averaging 3.28% and 4.98 to 6.35% with an average of 5.91% in mining and non-mining sites, respectively, were also observed in a similar investigation by Asamoah et al. (Asamoah et al., 2023). The low TOC levels at the study communities could be attributed mainly to mining operations and other diverse land activities, loss of vegetable cover, or organic matter contributions from the mining activities (Leul et al., 2023; (Asamoah et al., 2023). This has implications for metal availability in soils because it reduces organic matter's ability to bind metals (Kan et al., 2022). This can increase metal mobility, leaching, and runoff, thereby impacting water quality. Moreover, low TOC may affect plant growth, soil structure, and nutrient cycling in soil (Asamoah et al., 2023). Geographical factors have an impact on the effect of low TOC on element availability; hence, the reason for soil conservation strategies, vegetation restoration, and organic matter improvements (Asamoah et al., 2023; Odom et al., 2021).

4.3 Pollution Status

Table 4.3. Pollution assessment results of potential toxic elements (PTEs)

PTEs	Igeo	CF	ErF	PER
As	-1.3985	0.69962	1.73202	6.99615
Cd	8.65586	680.739	2182.1	20422.2
Co	1.96723	6.37666	16.8974	31.8833
Cr	-7.7511	0.03217	0.11329	0.06434
Cu	-2.1489	0.34384	1.07213	1.71922
Hg	-5.6239	0.04064	0.13239	1.62553
Mn	-2.1162	0.42568	1.11936	0.42568
Ni	-1.9679	0.38682	1.20029	1.93408
Pb	-2.6375	0.24962	0.75192	1.24811
Ti	-6.9007	0.05746	0.20667	0.05746
V	-7.0377	0.03437	0.1226	0.06873
Zn	-1.9543	0.41643	1.21139	0.41643
PERI				
Mean				1705.717
Min				0.057461
Max				20422.17

Contamination factor – CF; geo-accumulation index – Igeo; potential ecological risk (index) – PER(I); enrichment factor – Erf

Formatted Table

The study accounts for the major ecological risk indices: contamination factor, geo-accumulation index, potential ecological risk index, and enrichment factor, to assess the contamination status of potential toxic elements (PTE) of the artisanal small-scale galamsey centres in the region. These indices employ mass balance chemical modelling to estimate the toxic contamination and distribution limits in comparison with background values (Koka et al., 2019).

4.3.1 Contamination Factor (CF) Assessment

The Contamination factor measures the degree of pollution of potentially toxic elements in the soil samples in the study areas (Gyamfi et al., 2021). In Table 4.4, the derived values for the contamination factor are displayed.

Table 4.4 Results of Contamination Factors (CF)

PTEs	CF	Interpretation
As	0.69962	Low contamination
Cd	680.739	Extreme contamination
Co	6.37666	Extreme contamination
Cr	0.03217	Low contamination
Cu	0.34384	Low contamination
Hg	0.04064	Low contamination
Mn	0.42568	Low contamination
Ni	0.38682	Low contamination
Pb	0.24962	Low contamination
Ti	0.05746	Low contamination
V	0.03437	Low contamination
Zn	0.41643	Low contamination

The CF for As, Cr, Cu, Hg, Mn, Ni, Pb, Ti, V, and Zn based on Martin and Meybeck's (1979) classification scheme, are all less than one (1), indicating low contamination in the soil samples. However, the mean Cf for Cd and Co of the study area are 680.74 and 6.38, respectively. The CF-revered soil samples are extremely contaminated with Cd. The CF for Co showed moderate contamination of the soil in the study area. The extreme and high CF values for Cd and Co, respectively, aligned with the outcome values obtained in the study of Boateng et al. (2012) in the Obuasi area and were attributed to their association with the ore mined in the study area (Gyamfi et al., 2019). The other PTEs have comparatively lower CF values below 1, suggesting an uncontaminated study area. Hence, the Cd and Co contamination of the soil could be affirmed as a result of the

rapid erosion and weathering from exposure of the ore to the environment through the mining activities. The average contamination factor of the potentially toxic elements follows the increasing order: Hg < Ni < Pb < Cu < V < Cr < Ti < Zn < Mn < As < Co < Cd. The high CF for Cd and Co may pose serious risks to the ecosystem, wildlife, and human health (Jiang et al., 2017). It has been noted that Cd is known to have high contamination in Ghanaian soils (Asamoah et al., 2023).

4.3.2 Enrichment Factor (Erf)

Soil enrichment characterization enables the normalization of element concentrations in the soil to unitless "concentrations", which facilitates comparisons among several elements (Dartey & Gyamfi, 2024; Gyamfi et al., 2020). Enrichment factors may efficiently classify soils into contamination groups that are the same for all components, regardless of their relative abundance (Addai-Arhin et al., 2022). According to Zhang and Liu (2002), Erf values between 0.5 and 1.5 indicate that the metal is entirely from crustal materials or natural processes, whereas Erf values greater than 1.5 suggest that the sources are more likely to be anthropogenic.

Table 4.5. Enrichment factor (ErF)

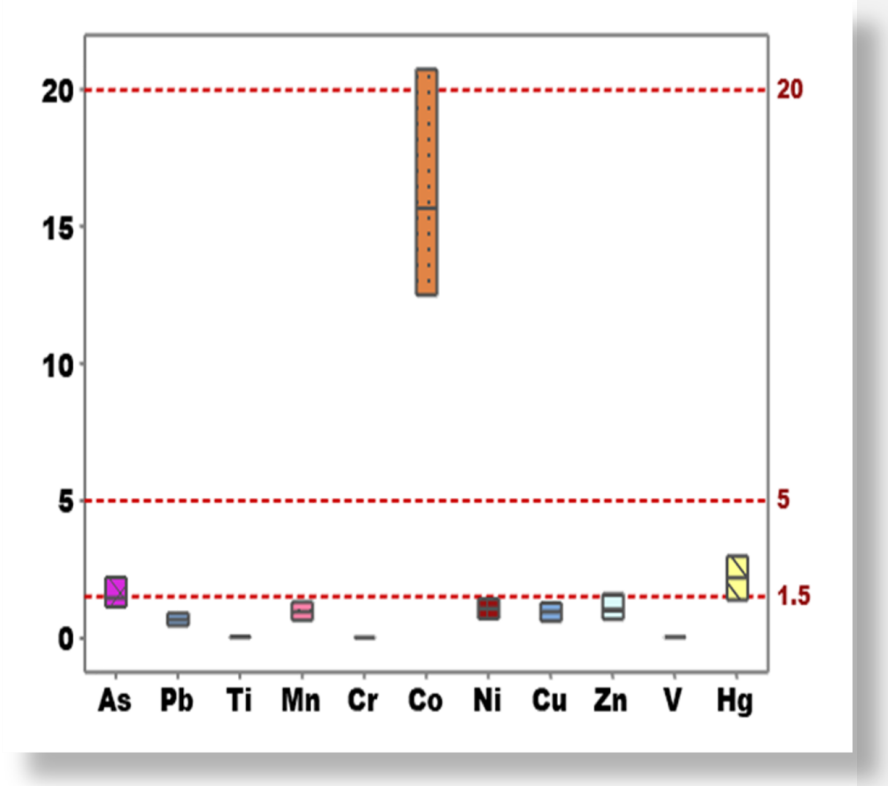

Figure 4.5 shows the enrichment factor of PTEs in soil samples of the study area, indicating a high enrichment with As, Cd, Hg, and Co. The Erf concentration of As, Cd, and Co were found to be greater than one (Erf > 1.5), predicting their source may be linked to anthropogenic activities.

The Erf mean for Cd showed an extremely high enrichment in the soil samples. The Erf value for Co was found within 5 < Erf > 20, suggesting a high enrichment in the study area. In addition, the Erf value for As and Hg were found within 2 < Erf > 5, indicating

a moderate enrichment of soil in the study area. The source of As, Hg, Co, and Cd enrichment means could be traced to Au-Ag mining and agricultural activities in the area. The remaining PTEs had their Erf mean below 1.5, which is insignificant to enrich the study area in their current state. Hence, these PTEs in the soil may enrich the study area over time due to their bioaccumulation and non-biodegradable nature.

4.3.3 Geo-accumulation Index (Igeo)

Table 4.6. Results of geo-accumulation index (Igeo)

PTEs	Igeo	Interpretation
As	-1.3985	Practically unpolluted
Cd	8.6559	Very Strongly polluted
Co	1.9672	Moderately polluted
Cr	-7.7511	Practically unpolluted
Cu	-2.1489	Practically unpolluted
Hg	-5.6239	Practically unpolluted
Mn	-2.1162	Practically unpolluted
Ni	-1.9679	Practically unpolluted
Pb	-2.6375	Practically unpolluted
Ti	-6.9007	Practically unpolluted
V	-7.0377	Practically unpolluted
Zn	-1.9543	Practically unpolluted

Table 4.6 displays the estimated geo-accumulation index for studied PTEs in the soil samples in the study area. The computed Igeo mean indication based on Muller (1969) of all the distinct soil regions for Pb, As, Zn, Cu, Fe, Mn, Cr, Ti, and Ni was less than the least reference Igeo value, forty (Igeo < 40), except for Cd. The lowest Igeo values indicate unpolluted soil in the study areas. The Igeo concentration of Cd was 8.66. The Igeo value for Cd indicates the very high pollution soil of the study area. The very high

Igeo values for Cd aligned with the outcome values obtained in the study of Asamoah et al., (2023) and Boateng et al. (2012) areas in Ghana. The Igeo results were attributed to have been influenced by ore mined in the study area (Gyamfi et al., 2019). However, the study area is prone to further contamination over time due to the bio-accumulation characteristics of these PTEs in the soil in the study area (Jin et al., 2019; Nkansah, Darko, Dodd, Opoku, Bentum Essuman, et al., 2017)

4.3.4 Potential Ecological Risk (PER) and Index (PERI)

Table 4.7. Results of Potential Ecological Risk (PER) and Index (PERI)

PTEs	PER	Interpretation
As	6.9961538	Low Risk
Cd	20,422.17	Very High Risk
Co	31.8833	Low Risk
Cr	0.0643419	Low Risk
Cu	1.7192165	Low Risk
Hg	1.6255333	Low Risk
Mn	0.4256804	Low Risk
Ni	1.9340781	Low Risk
Pb	1.248109	Low Risk
Ti	0.0574606	Low Risk
V	0.0687337	Low Risk
Zn	0.4164305	Low Risk
	PERI	
Mean	1705.71714	Very High Risk
Min	0.05746065	
Max	20422.1667	

The potential ecological risk and the potential ecological risk of As, Cd, Co, Cr, Cu, Fe, Hg, Mn, Ni, Pb, Ti, V, and Zn values were calculated from all the different soil samples in the Atwima Mponua District and are shown in Table 4.7. The PER values of As, Co, Cr, Cu, Hg, Mn, Ni, Pb, Ti, V, and Zn in the study areas range from 0.09 to 10.37,

representing a very low potential risk area compared to the reference value (PER < 40). However, the mean ecological risk (PER) value of Cd in the soil samples was 20422.17. This predicts an extremely high potential ecological risk (PER ≥ 320) in the study communities. The findings are also consistent with the PER values published by Kabir et al (2022), (Lin et al., 2017), and (Najmeddin et al., 2017) indicating a high ecological risk of cadmium. Therefore, cadmium poses a very significant ecological risk to the local environment, prompting the implementation of protective measures in sensitive areas (Kabir et al., 2022). However, the outcome indicates that the PTEs in the soil may not endanger the immediate ecosystem, except for cadmium. The average ecological risk values followed the descending order as Cd > Co > As > Cu > Pb > Mn > Ni > Hg > Zn > Cr > V > and Ti. The assertion is hypothetically proven that Cd is known to have high concentrations in Ghanaian soils (Asamoah et al., 2023).

The assessed potential ecological risk index (PERI) of PTEs in soil is displayed in Table 4.7. Shown an average value of 214.04. This indicates moderate ecological risk (150 ≤ PERI < 300) across the study area. The PERI for soils of Atwima Mponua District established that the area has been contaminated by PTEs, impacting negatively on the ecosystem. As a result of this, the authorities must take the necessary action to reduce the contamination of the environment by potentially toxic elements. Cadmium is the major environmental risk contributor, contributing 99.3% of the ecological risk on average. This makes Cd the element that contributes largely to the ecological risk across the study area. Cobalt and arsenic contribute 0.4% and 0.1% respectively of the PERI on average, making them the second and third highest contributors. The remaining elements

contribute to an average of 0.2%, suggesting that their presence may likely not pose any danger to the communities.

4.4 Spatial Distribution of Potential Toxic Elements

Figure 4.7. displays the results of the spatial spread of potential toxic elements (PTEs) in the study area. The concentrations of vanadium and cadmium showed extremely high distribution in almost the entire study area, except for a substantially small portion at the northeast locations that recorded low to moderate levels.

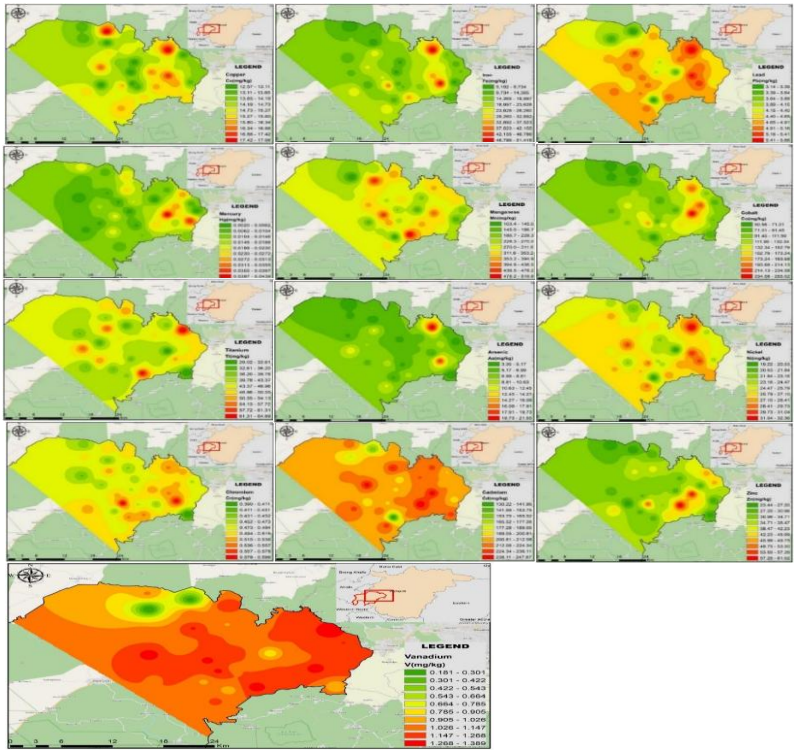

Fig. 4.1. Spatial Distribution Maps for PTEs in the Soil of Atwima Mponua District

However, the concentration of moderate to very high concentrations was observed for Ni, Cr, Mn, Cu, and Ti in the greater portions of the study regions, except for a few portions of the northern parts of the middle belt of the study area. Additionally, the north to north-west parts of the study area reported very low to low concentrations of zinc, cobalt, iron, and mercury, which, in contrast, showed a moderate to very high concentration of these PTEs at the eastern and western portions of the study area. Finally, arsenic was found to have a very low concentration at the northern and western areas, with a low to medium concentration at the central to northern regions. High to very high levels were found in the eastern portions of the study area.

4.5 Source Apportionment

Positive Matrix Factorization (PMF) is an advanced receptor model used for source apportionment of environmental pollutants (Jiang et al., 2017), particularly heavy metals in air, water, and soil. The technique decomposes the observed concentration matrix into factor contributions and factor profiles, helping identify pollution sources and their respective contributions (Brown et al., 2015; Hossain Bhuiyan et al., 2021). The given results include factor fingerprints, factor profiles, and regression diagnostics from a Fpeak PMF run, which we analyze to determine the major sources of contamination (Brown et al., 2015; Epa & Exposure Research Laboratory, 2021).

4.5.1 Positive Matrix Factor (PMF) and Enrichment Factor (EF)

PMF outputs validate factor analysis to apportion the sources of PTE contamination in soil. The correlation coefficient of determination (R^2) was kept at > 0.60 to measure the goodness of fit (QT) of the results (Hossain Bhuiyan et al., 2021). Most species exhibited

high R^2 values (close to 1.000) as in Fe, while As, Cd, Mn, and Ti also have high values > 0.96 indicating predictive correlation. These heavy metals are linked to crustal material sources (Jiang et al., 2017).

Table 4.8. Regression diagnostics from FPeak Run 3

Species	Intercept	Slope	SE	R2	KS Test Stat	KS Test P Value
Ti	0.516908	0.988827	0.283009	0.99937	0.111356	0.288141
V	1.256203	0.182214	0.257381	0.037498	0.133082	0.126185
Cr	0.494953	0.054711	0.056654	0.015179	0.198386	0.004311
Mn	38.1356	0.883961	19.48832	0.926505	0.09152	0.530723
Co	97.33258	0.215235	19.4537	0.286792	0.182345	0.011178
Ni	8.855642	0.645457	1.886832	0.655909	0.138214	0.101564
Cu	9.23869	0.360728	1.552762	0.166233	0.075881	0.760157
Zn	24.43933	0.353613	6.234291	0.3161	0.127716	0.156935
Hg	0.004719	0.000369	0.001092	0.009749	0.24806	0.000136
As	0.836781	0.931244	0.417524	0.994657	0.117191	0.234348
Pb	3.490389	0.256741	0.448672	0.078621	0.094329	0.491359
Cd	6.271428	0.970691	5.522683	0.967324	0.234163	0.000386
Fe	-0.14341	1.000001	0.175782	1	0.180856	0.012162

Statistical Diagnostics from a Fpeak PMF Run: Slope, Standard Error (SE), R2, Kolmogorov-Smirnoff (KS test) Statistics, and P-values

P-values and KS Test statistics assessed whether the residuals follow a normal distribution (Jiang et al., 2017). The higher p-values, as in Mn (0.531), indicate a better fit to normal distributions. And the low p-value (< 0.05) suggests that the residuals deviate significantly from normality as shown in Cd (0.000386) and Hg (0.000136). Elements with lower R^2 (Cr = 0.0157, Cu = 0.1662, Co = 0.2867) suggested that these species may have complex source contributions or measurement uncertainties (Jiang et al., 2017; J. Yang et al., 2022). The high R2 values for elements Fe = 1.0000, Cd = 0.9673, As = 0.9947, and Mn = 0.9265 indicated a strong fit of the PMF model to

observed data. Elements like Hg (p = 0.000136), Co (0.01178), and Cd (p = 0.000386) indicate statistically significant deviations, suggesting the need for refined modelling or additional source assessment (Hossain Bhuiyan et al., 2021). The elements Mn (p = 0.5307) and Pb (p = 0.4913) show better alignment with modelled sources.

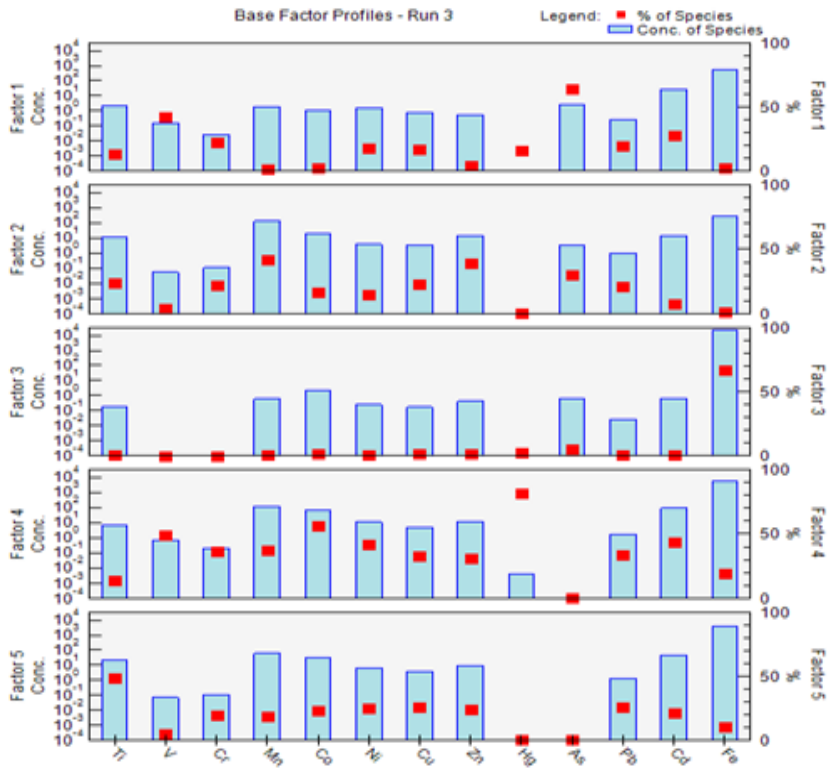

Figures 4.2. Base Factor Profiles – Run 3

Factor 1 concentrations were highly dominated by Iron (Fe) and Manganese (Mn) and sub-dominated by vanadium, chromium, copper, zinc, arsenic, lead, and cadmium with

a sum loading of 4.9%. This could indicate natural sources (lithogenic origin) and anthropogenic (mining activities) (Hossain Bhuiyan et al., 2021; Jiang et al., 2017)

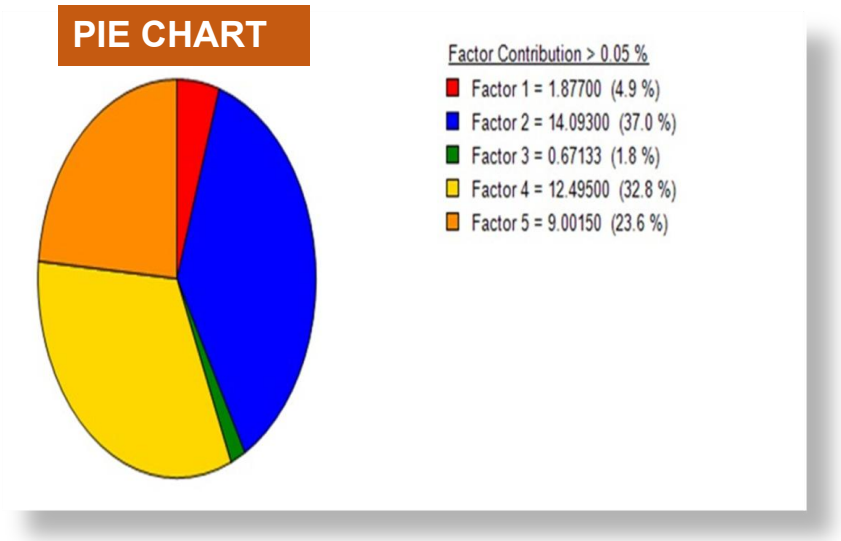

Figure 4.3. Factor Contribution > 0.05%

S**ource 1 (Red)** in Fig. 4.14 showed a sub-dominance of V (20) %, Cr (11) %, Fe (5.5) %, Cu (5.5) %, and Zn (3.5) %. Thus, arsenic (As = 100%) in source 1 represented the main dominant source of pollution, establishing that the origin of As emanated from ore mining, pesticides, and combustion (anthropogenic sources) (Jiang et al., 2017). However, the value of the enrichment factor for As is below one (ErF < 1.5) as shown in Table 4.3, indicating natural sources. Meanwhile, (Hossain Bhuiyan et al., 2021) claim that arsenic pollutes groundwater, air, and irrigation and might contribute to the high accumulation in soils. Literature 2.2 reviews that ore mining, combustion, smelting,

deposition of atmospheric aerosols, pesticides, and biosolids may all contribute to the build-up of As in soils.

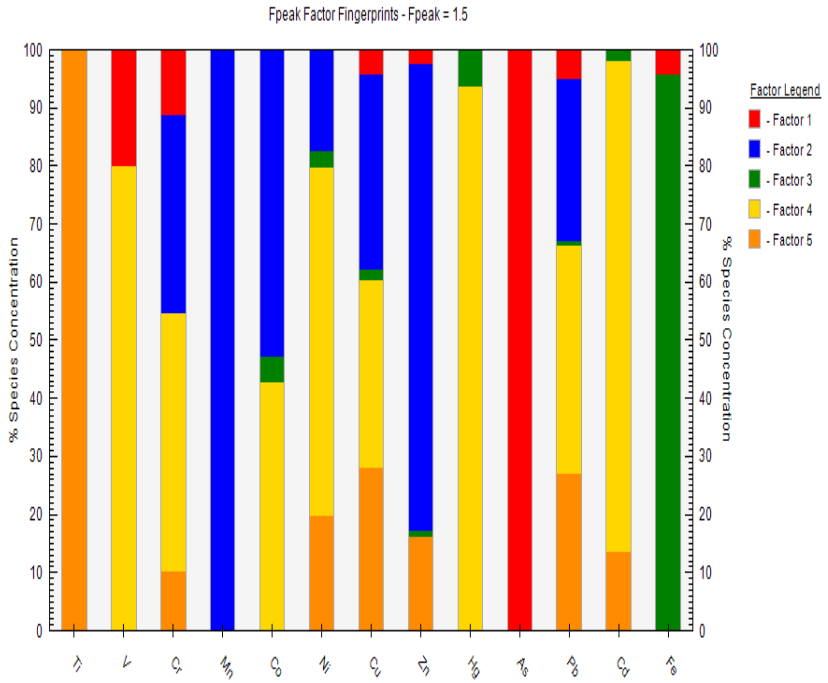

Figs. 4.4 Factor Finger Print (Fpeak = 1.5) Contribution Panel

Factor 2 shows high dominants of Mn, Co, Zn and sub-influenced by Cr, Ni, Cu, Hg, and Pb, with a total loading of 37.0% indicating their association with vehicular source Au-Ag mining activities (anthropogenic).

Source 2 (Blue) recorded a sub-dominance of Cr = 34%, Ni = 18%, Cu = 29.5%, Pb = 18% and was primarily dominated by Mn – 100%, Co – 52%, and Zn – 72.5% as shown in the figure print panel. The enrich factor (ErF) for Mn and Zn was below the background value of 1.5, suggesting their contribution is likely to emanate from the

geogenic sources (Hossain Bhuiyan et al., 2021; Qin et al., 2021). However, previous works in Table 2.2 suggested that Mn and Zn predict their origins from ore mining, vehicular emissions, and iron and steel industries. These anthropogenic emanations may be spread in the investigation area through geogenic activities (Hossain Bhuiyan et al., 2021). In addition, the ErF for Hg and Co > 1.5 shown in Table 4.3 affirms the likelihood of the anthropogenic source of apportionment. Again, the studied literature in (2.1 and 2.2) suggested that the source of Co is traced to Au-Ag mining, sewage sludge, phosphate fertilizers, smelting of cobalt ores, processing of cobalt alloys, and burning of fossil fuels. Whereas Hg which is most likely to be traced to mining activity during their gold amalgamation. My field observation revealed that this study region is linked to several Au–Ag mines, which may be the main Co source of pollution in the area (Najmeddin et al., 2017)

Factor 3 was highly characterized by Fe and substantial fluctuations of Co, Ni, Cu, Zn, Pb, and Cd, with the lowest sum loading of variance 1.8%, indicating the hypothesis could be predicted as natural soil (lithogenic origin) or rock-derived source (Yang et al., 2022).

Source 3 (Green) produced a sub-dominance by Hg = 5.8%, Co = 5%, Cd = 5 %, Cu = 3%, and Pb = 0.5% as shown in figure print panel. The heavy metal, iron (Fe = 94.5%) represents the principal dominant in source 3, suggesting that iron may have originated from a lithogenic or rock-derived source (Hossain Bhuiyan et al., 2021; Jiang et al., 2017). The enrichment factor (ErF) for iron (Fe) was less than unity (Table 4.3), affirming that iron may have originated from a natural source.

Factor 4 was uniformly distributed with peaks from mercury, cadmium, cobalt, vanadium, chromium, nickel, copper, and lead, predicting the emission from Au-Ag

mining and agricultural activities, and is widely associated with electroplating industries (Hossain Bhuiyan et al., 2021; Jiang et al., 2017) (anthropogenic sources).

The **source 4 (Yellow)** in Fig. 4.14 contributions were defined as 96.2% mercury, 80% cadmium, 80% vanadium, 60% nickel, 50.5 % lead, 43% cobalt, 43.8 % copper, and 44.5 % chromium with 2nd highest of sum variance of 32.8% contributions, indicating the Au-Ag mining, agricultural activities and combustion (Jiang et al., 2017; Najmeddin et al., 2017) as the main sources. Additionally, the enriching factor for Co and Hg was greater than one and a half (ErF > 1.5), especially Cd (1,099.496), recording exceedingly higher. This confirms the contribution is likely to emanate from anthropogenic sources (Hossain Bhuiyan et al., 2021) primarily, Au–Ag mining (Konadu et al., 2023; Snow et al., 2021). Although previous research has proposed that emissions from ore mining, combustion, agricultural activities, biosolids, industrial waste, electroplating, cobalt ores, smelting, and lubricants (Delower Hossain et al., 2020) could be the cause of the Co, Hg, Cd, Cu, Pb, Zn, and Ni contamination in soil (Yang et al., 2022; Yang et al., 2021). However, the field observation revealed that the area is connected to thousands of Au–Ag mining (galamsey), which may be the main anthropogenic sources of pollution among the suggested sources in the study area.

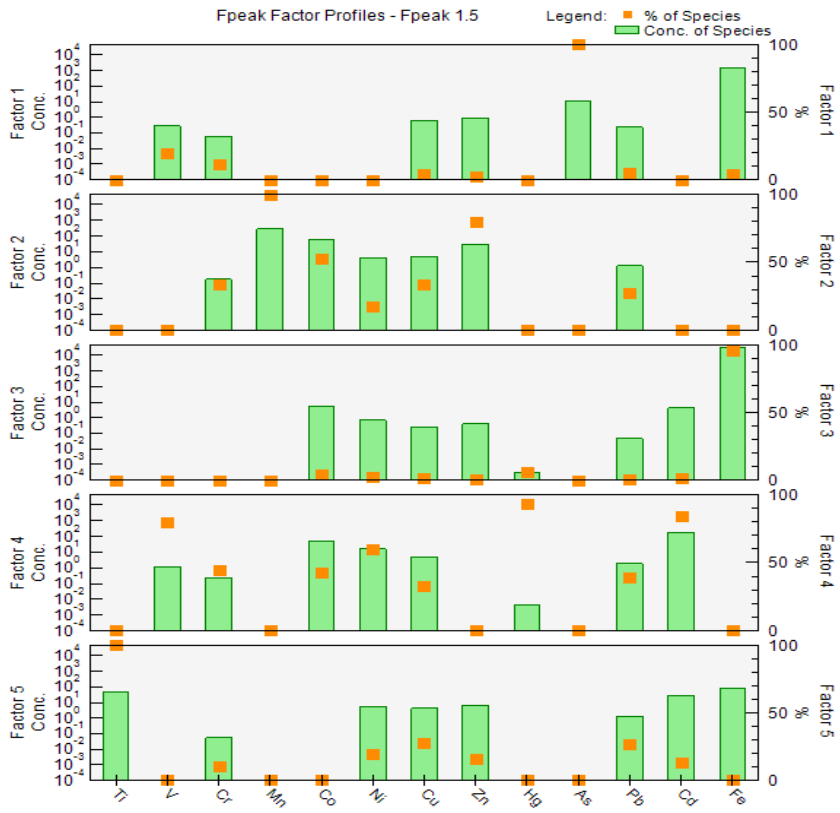

Figures 4.5. Fpeak 1.5 source profile panel

The fifth and 3rd highest **factors** accounted for 23.6% of the total variance, have a moderate concentration for Ti and Ni, and are sub-influenced by Cu, Pb, Zn, Cr, and Cd. This suggests that Ti and Ni may be emanating from weathering (lithogenic) sources (Jiang et al., 2017).

Source 5 (Red) revealed a sub-dominance of Cu (29%), Cr (43%), Pb (27%), Cd (14.5%), and Zn (22.3%), as shown in the figure print panel. The elements Ti (100%) and Ni (60%), in source 5, represented the main contributing source. This affirms that the source of pollution originates from soil-derived weathering (lithogenic) sources

(Delower Hossain et al., 2020; Hossain Bhuiyan et al., 2021). Several studies, including Asamoah et al., 2023a; Jiang et al., 2017; and Konadu et al., 2023, have noted that Ti and Ni probably originate from natural sources. The prediction was also confirmed by the enrichment factor, which established Ti and Ni below one (ErF > 1.5), as shown in Table

4.6. Pearson's Correlation Assessment of PTEs in Soil.

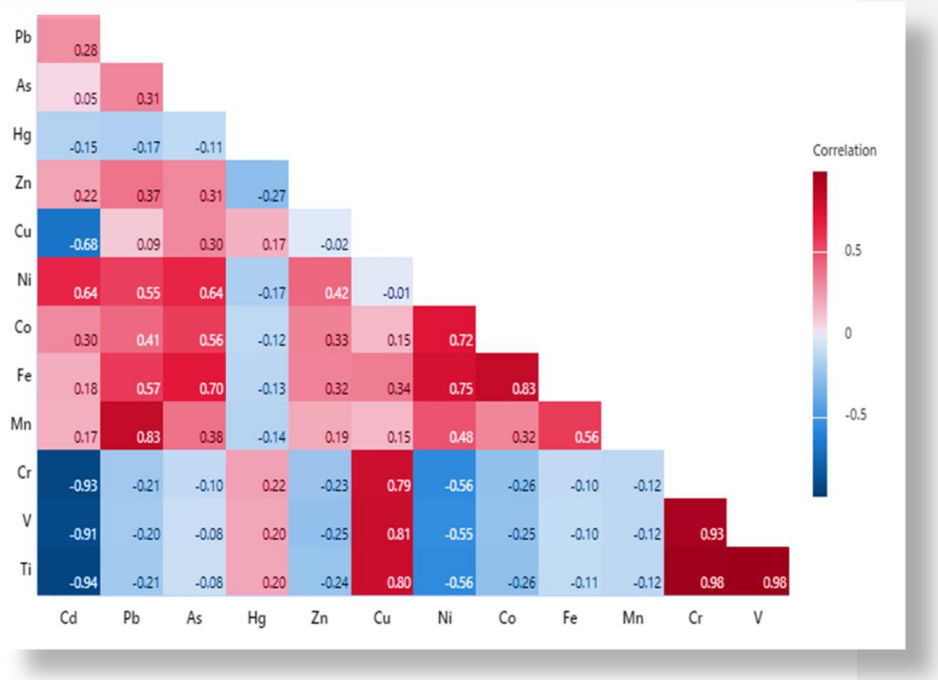

Correlation is significant at the 0.05 level (2-tailed), $\alpha < 0.05$

Figure 4.6. Pearson's Correlation

Pearson correlation coefficient (r) analysis was utilized to examine the relationships between the concentration of PTEs in the research region. The correlation results are displayed in Table 4.7. In this study, correlation coefficients > 0.8, 0.6 < r < 0.8, and < 0.6 were regarded as strong, moderate, and weak correlations, as described by (Dartey &

Gyamfi, 2024). The geology of a region greatly influences its environmental chemistry (Dartey & Gyamfi, 2024; Konadu et al., 2023). Chemical ions in the environment, including many metallic ions, are attributed to both anthropogenic and geogenic sources. However, the concentrations of potentially toxic elements in the reference sample used in this study suggest that the heavy metals could not be linked to geogenic sources, since there are no geologic deposits rich in the PTEs under analysis. Co has a weak positive association with Cd, Pb, As, Hg, Zn, and Cu with a weak positive High connection with Ni. A positive correlation was established between As, Cd, and Pb. Zinc recorded a weak correlation with Cd, Pb, As, and Hg. Lead established a weak positive correlation with Cd. A positive weak correlation was also recorded between Cu, Cd, Pb, As Hg, and Zn. Mercury has a moderate correlation with Cd and a weak positive association with Pb and As. Nickel has a strong positive link with Hg and a moderate correlation with Cd and As. And a weak positive association with Pb, Zn, and Cu.

Iron has a weak positive correlation with Cd, Pb, Zn, and Cu and a high positive correlation with Hg, Ni, and Co. Manganese has a weak association with Cd, As, Hg, Zn, Cu, Ni, Co, and Fe. It also has a strong positive correlation with Pb. Chromium established a weak negative correlation with Hg, Zn, Ni, Co, Fe, and Mn. A moderate negative association was also established between Mn and Cu. It further showed a strong positive correlation between Mn and Cd, pointing to a natural and anthropogenic source as the traces of common origination. Vanadium has a weak negative link to Pb, As, Hg, Zn, Ni, Co, Fe, and Mn with a high positive link to Cu and Cr as well as a high negative association with Cd. Finally, Ti has a weak correlation with Pb, As, Hg, Zn, Ni, Co, Fe, Mn, and V. A high negative correlation was also shown between Ti and Cd. Additionally,

a high positive association was further established between Cu, Cr, and Ti. The Au-Ag mining, agricultural activities, and lithogenic sources of the potentially toxic elements in the soils may be the common sources of origination.

4.7. Principal Component Analysis (PCA)

PCA model characteristics were produced from the summarized components, accounting for 86.2% of the total variance. This multivariate analytical method assisted in finding potential sources of toxic elements (PTE) contamination sources in the soils of the investigated area. Four principal components (PCs) were identified, with eigenvalues greater than 1 through varimax rotation.

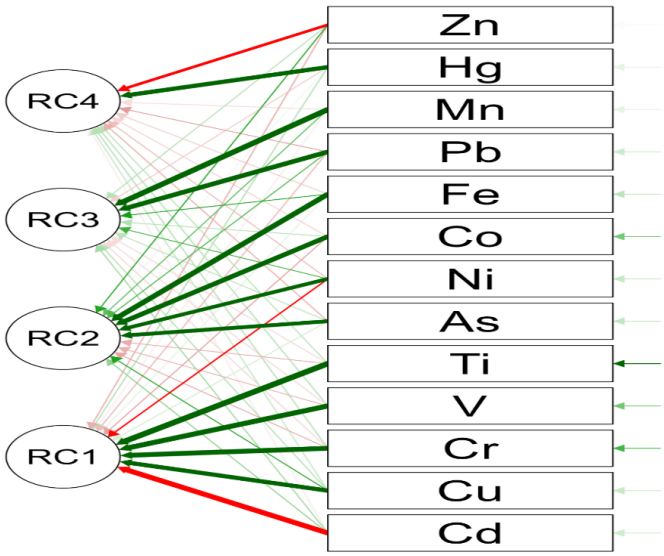

Figure 4.7. Path diagram of the principal components

Tables 4.6, 4.7, and Figure 4.17 illustrate the primary elements of the outcomes of the investigation. The 1st principal component (PC1) showed an accumulated component characteristic of 36.2%, as the highest sum loading variance. The recorded heavy metals were Ti, V, Cr, Cu, Ni, and Cd with component loadings (coefficients) of low 0.44 to high value of 0.98. The component loadings for heavy metals Co, Ni, and Zn were negatively correlated with PC1 and PC4, respectively, indicating that their lower concentration in the soil leads to the rise concentration of other variables and vice versa (Suryawanshi et al., 2016). Component 1 showed strong positive associations between Ti, V, Cr, Cu, and Cd signalling traced to anthropogenic activity sources. This may include small-scale mining (galamsey) activities, combustion of fossil fuel, biosolids (sewage sludge), and other agricultural activities in the study site.

Principal component two (PC2) was dominated by nickel, cobalt, arsenic, and Iron with the component loading (coefficients) of -0.78, 0.87, 0.82, and 0.87, respectively. Their sum component characteristics of variances were 25.0% which was the 2nd highest factor, indicating their sources from both lithogenic and anthropogenic origins.

The principal component three (PC3) showed variable loadings (coefficients) of 0.89 and 0.92, respectively. This factor had Mn and Pb as the dominant elements. It was the 3rd highest explained accumulated variance characteristic of 15.0%. Their sources of pollution could be linked to anthropogenic sources. Finally, component four (PC4) is dominated by Hg and Zn elements. This PC explains 9.8% of the total variance and suggests the heavy metals may have come from ore mining, pesticide, and combustion sources.

Table 4.9 Component Loadings

	Component Loadings				
	PC1	**PC2**	**PC3**	**PC4**	**Uniqueness**
Ti	0.979				0.010
V	0.964				0.040
Cr	0.962				0.041
Cd	-0.934				0.074
Cu	0.869				0.098
Ni	-0.443	0.779			0.091
Fe		0.866			0.104
Co		0.862			0.217
As		0.822			0.293
Mn			0.924		0.080
Pb			0.892		0.087
Hg				0.872	0.219
Zn				-0.641	0.438

Note. The applied rotation method is varimax.

Table 4.10. Component Characteristics

Component Characteristics

	Unrotated solution			**Rotated solution**		
	Eigenvalue	**Proportion var.**	**Cumulative**	**SumSq. Loadings**	**Proportion var.**	**Cumulative**
Component 1	5.532	0.426	0.426	4.706	0.362	0.362
Component 2	3.530	0.272	0.697	3.250	0.250	0.612
Component 3	1.119	0.086	0.783	1.971	0.152	0.764
Component 4	1.027	0.079	0.862	1.280	0.098	0.862

PC1, accounting for the highest variance (36.2%), revealed strong positive loadings of Ti, V, Cr, Cu, and Cd, indicating that these elements likely originate from a common anthropogenic source, particularly artisanal small-scale mining (ASM), agricultural runoff, and fossil fuel combustion (Hossain Bhuiyan et al., 2021; Qin et al., 2021). The

negative correlations observed for Cd and Ni within this component further suggest competitive interactions or differing mobilities in the soil environment. Despite the geogenic signal for Ti, V, and Cr as indicated by their enrichment factors (Erf < 1.5), the significant presence of Cd both with Erf > 1.5, establishes the dominant influence of anthropogenic activities. My field observation revealed that this study region is linked to thousands of Au–Ag mines, which may be the main anthropogenic source of pollution in the area.(Najmeddin et al., 2017).

PC2 showed a very strong positive correlation with As, Co, Fe, and Ni, predicting their similar source of origin. PC2 aligned with the positive matrix factorization (PMF) sources contribution 1, where As part took 100% dominance. The enrichment factor for Ni was below the background value (Erf < 1.5) unity suggesting their contribution is likely to emanate from the geogenic sources (Hossain Bhuiyan et al., 2021; Qin et al., 2021). However, the Erf for As and Co were greater than one (Erf > 1.5), as shown in Table 4.5, which affirms the likelihood of the anthropogenic source of apportionment. Additionally, the literature in 2.5.9 and 2.5.6 suggested the source of As and Co could be traced to Au-Ag mining, pesticides, sewage sludge, phosphate fertilizers, smelting of cobalt ores, processing of cobalt alloys, and burning of fossil fuels. My field observation revealed that this study region is linked to thousands of Au–Ag mining whose activities may be the main anthropogenic source of pollution in the area (Najmeddin et al., 2017).

PC3, contributing 15% to the total variance, showed strong associations between manganese (Mn) and lead (Pb). These elements are commonly associated with metal ore bodies and may be released through ore weathering and mechanical disruption during

mining (Hossain Bhuiyan et al., 2021; Qin et al., 2021). Despite their lower enrichment values (Erf < 1.5), suggesting a geogenic origin, the anthropogenic disturbance through mining activities likely enhances their mobility and bioavailability in the soil matrix (Lal et al., 2021). Thus, the Mn and Pb in the area could be a result of rapid erosion and weathering from exposure of the ore to the environment through artisanal small-scale mining activities.

Principal component four, 9.8% of the variance, was characterized by mercury (Hg) and zinc (Zn). The strong correlation of Hg with this component supports its association with ASM, particularly the use of mercury in gold amalgamation processes. Conversely, Zn's negative loading may indicate a dilution effect or differing mobility under the prevailing soil conditions. Given that Hg had an EF > 1.5 while Zn did not, this component further emphasizes the selective anthropogenic influence on heavy metal dynamics. However, the Erf for Hg was greater than one (Erf > 1.5), as shown in Table 4.5, which affirms the likelihood of the artisanal small-scale mining source of apportionment. Furthermore, the literature in 2.5.11 suggested that the source of Hg could be linked to small-scale mining (galamsey) operations and agricultural activities in the area.

Thus, the PCA results align with this study that employed multivariate statistical techniques (PMF) to distinguish between natural and anthropogenic sources of soil contamination (Najmeddin et al., 2017). In this context, PCA, complemented by enrichment factor analysis and supported by field observations, proved the dominant processes affecting soil quality in mining-impacted areas (Jiang et al., 2017; Yang et al.,

2022). In addition, the identification of distinct sources linked to ASM, agrochemical use, and fossil fuel combustion highlights the multifaceted nature of environmental contamination in the district. The strong associations observed between certain metals also suggest potential synergistic toxicity, which may have implications for ecological and human health, particularly in areas of co-contamination (Armah et al., 2010).

4.8. Human Health Risk Assessment

The results of the human health risk assessment provide critical insight into the potential adverse effects of potentially toxic elements (PTEs) (Jiang et al., 2017) on populations residing in the artisanal small-scale mining (ASM) areas of the Atwima Mponua District. Through the evaluation of exposure pathways (ingestion, inhalation, dermal contact), and, in the case of mercury (Hg), (vapourization) the study demonstrates that both non-carcinogenic and carcinogenic health risks are present, with children disproportionately affected.

4.8.1 The Hazard Quotient (HQ) and Hazard Index (HI

The hazard quotient is a metric employed to assess the potential risk to human health posed by a specific element. The HQ > 1 indicates that there is a likelihood of potential risk associated with that element's exposure, whereas HQ < 1 represents no likelihood of risks for exposed populations. The hazard quotient and hazard index of the PTEs (As, Cd, Co, Cr, Cu, Fe, Hg, Mn, Ni, Pb, Ti, V, and Zn) were assessed because of their relatively strong toxicity to human health (Jiang et al., 2017).

Table 4.11. The quantitative analysis for non-carcinogenic Health Risk

	HQ INH.		HQ ING.		HQ DERM.		HI	
PTEs	**C**	**A**	**C**	**A**	**C**	**A**	Children	Adults
As	8.30E-12	1.10E-11	0.08532	0.01828	0.19721	0.03109	0.38307	0.07092
Cd	2.60E-11	3.30E-11	0.15521	0.06652	24.6415	3.88438	24.7967	3.9509
Co	2.60E-11	3.30E-11	6.61613	1.41774	2.87802	0.45368	9.49414	1.87142
Cr	2.00E-14	2.60E-14	0.00112	0.00024	0.00048	7.60E-05	0.0016	0.00032
Cu	4.60E-14	5.90E-14	0.00995	0.00213	0.00361	0.00057	0.01355	0.0027
Mn	7.30E-11	9.40E-11	0.05299	0.01136	0.02305	0.00363	0.07604	0.01499
Ni	1.60E-13	2.00E-13	0.17681	0.15155	0.07691	0.01212	0.25372	0.16367
Pb	1.70E-13	2.10E-13	0.06591	0.02825	0.02631	0.00415	0.09222	0.0324
Ti	1.10E-13	1.40E-13	0.00374	0.00022	0.00044	6.90E-05	0.00418	0.00029
Zn	1.60E-14	2.10E-14	0.00087	0.00019	0.00189	0.0003	0.00276	0.00048
V	1.40E-14	1.90E-14	2.60E-05	5.60E-06	1.10E-05	1.80E-06	3.80E-05	7.40E-06

HQ – Hazard Quotient; HI – Hazard Index; C – Children and A – Adults

The total hazard index (THI) is shown in Figure 4.17. Values were 35.89 and 6.30 for children and adults, respectively. Values greater than one (THI > 1) indicate that the communities may experience non-carcinogenic (Jiang et al., 2017; Konadu et al., 2023) health risks. Children are more likely to be exposed to higher hazard risk than adults. This assertion was comparatively affirmed by (Asamoah et al., 2023; Gyamfi et al., 2021). Among the estimated PTEs, the hazard quotient (HQ) values for Manganese via ingestion pathway exceeded 1, which accounted for 18.45 % and 22.54% of THI for children and adults, respectively. Again, the results of the HQ values for Cd and Mn via the dermal contact route exceeded 1, accounting for 68.65% and 8.02 % of THI for children and adults, respectively. Additionally, the HQ value of Cd through the dermal route is estimated at 61.59% of THI for adults. The HQ indices for heavy metals followed the order: dermal contact > soil ingestion > air inhalation. Through every channel about each element, children have higher non-carcinogenic risks than adults across the study area, suggesting that they are more vulnerable to environmental pollutants. Children's physiological and behavioural traits, such as their hand-to-mouth actions in soil and their increased respiration rates per unit body weight, may be responsible for this vulnerability. The danger associated with all PTEs in soil was similar for each pathway, as the results were consistent with the study by (Gyamfi et al., 2021) whose investigation was on contamination, exposure, and risk assessment of mercury in the soils of an artisanal gold mining community in Ghana and was reiterated by (Jiang et al., 2017; Odukoya et al., 2018).

4.8.2. Carcinogenic Health (Lifetime Cancer) Risk Assessment in Soil

The estimated values for the lifetime cancer risk (CR) and total cancer risk (TCR) for the elements (arsenic, chromium, lead, and cadmium) through oral, cutaneous exposure, and inhalation routes for children and adults are shown in Figure 4.19. The TCR values for children and adults were 8.921×10^{-4} and 1.997×10^{-4}, respectively. The total carcinogenic risk for both children and adults were high than the maximum tolerable or acceptable risk value (1×10^{-4}) (Jiang et al., 2017), indicating that, the populates in the study area are more likely to be affected by the high life cancer risk, establishing children are more vulnerable than the adults. However, the TCR value of As for both children and adults was extremely highly tolerance limit, indicating extremely higher life time carcinogenic risk in soil of the study area. The trend of TCR values for different heavy metals increased in the order as: Cr < Pb < Cd < As. The cancer risk (CR) values of As, Pb, and Cd for both children and adults, through the ingestion pathways were above the negligible risk level of 1×10^{-6}, but lied within the life cancer risk tolerance limit, indicating low significant cancer effects on the peoples. The CR value of Cr for adults across all the pathways stood in acceptable risk limit, while the CR value of Pb for adults was below the negligible risk level of 1×10^{-6}, indicating no significant cancer risk. These findings align with results from studies conducted in other contaminated environments by (Dartey & Gyamfi, 2024), and the mining community by (Odukoya et al., 2018) emphasizing the persistent challenge of PTE induced carcinogenicity in environmental health research.

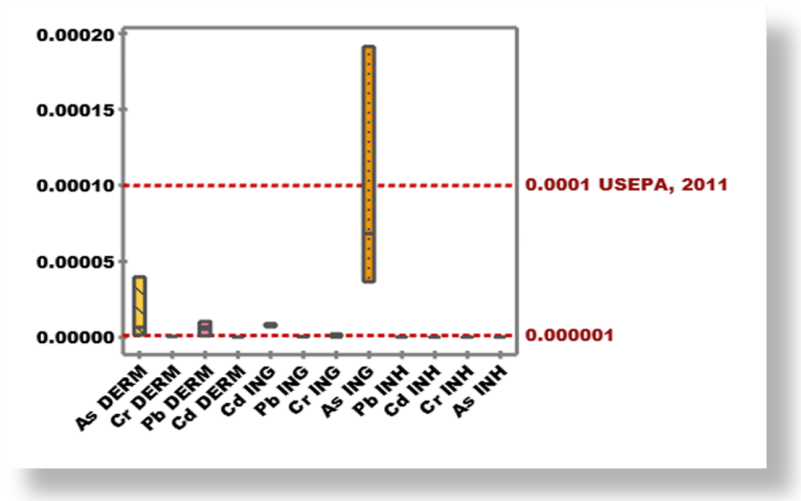

Figure 4.8. Estimation of Carcinogenic Health Risk in Soil

4.9 Non-carcinogenic and Carcinogenic Risk Assessment of Mercury (Hg)

Table 4.12. Hazard Quotient (HQ) and Hazard Index (HI) of Mercury (Hg) in Soil.

Hg	HQing	HQinh	HQder	Hqvap	HI
Children	0.00924	4.3E-13	0.84272	0.05312	0.90508
	0.00396	5.6E-13	0.18058	0.02996	0.2145

Hazard Quotient (HQ): Hazard Index (HI): Mercury (Hg)

The hazard quotient (HQ) and hazard index (HI) for non-carcinogenic risk were calculated for mercury (Hg) exposure through Ingestion (ing), inhalation (inh), skin contact (der), and vaporization (vap) pathways as displayed in Table 4.9. and Figure 4.9. While the hazard quotient (HQ) values for Hg remained below 1, indicating the study area is not contaminated with Hg at its current state. However, among the below HQ

values of Hg, children and adults' HQ (0.84272) via dermal routes was approached the critical threshold, predicting that ASM activities are more likely to pose risks if the intensity of pollution sources are not checked. This is particularly worrisome given Hg's well-documented neurotoxicity and bioaccumulation potential (*WHO Global Strategy on Health, Environment and Climate Change*, 2020). Furthermore, the mean HQ value for children via dermal route suggests children in the study area would be more vulnerable to high risk because of their desire to touch artisanal small-scale mining soil with bare hands and the frequent hand-to-mouth contact without resorting to proper personal hygiene conduct (Albert et al., 2021; Rinklebe et al., 2019). The findings echo the results of (Addai-Arhin et al., 2022) and (Albert et al., 2021), who emphasized the risks posed by mercury exposure in artisanal mining communities. The HQ values for Hg followed the increasing order as: Inh < Ing < Vap < Derm. This HQ order is in line with a study done at Obuasi, a small-scale gold mining site by (Addai-Arhin et al., 2022).

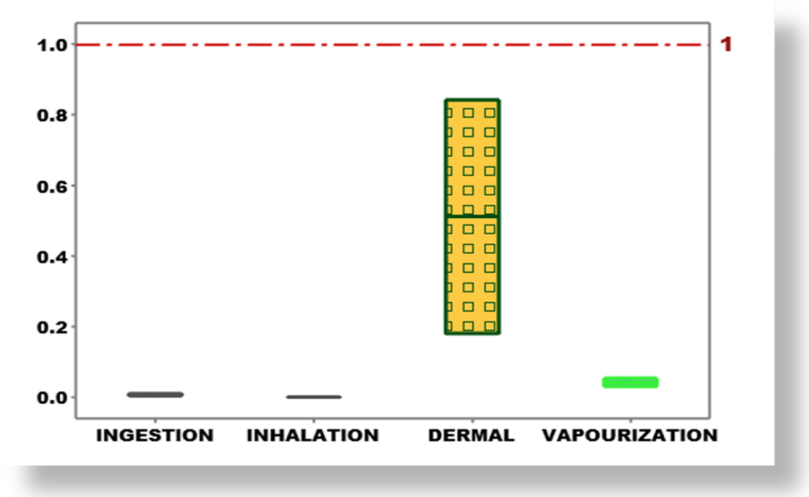

Figure 4.9. Total Health Risk Index (HI) for Mercury in Soil

The mean results for carcinogenic hazards index (HI) for children and adults in the study area were also lower than unity (HI < 1). This HI for values suggests the study area is free from Hg contamination at its current state. However, the Hg value for children (0.905) was close to reference value 1, suggesting the Hg potential to contaminate the study area if the same activities persist. Again, children are at a higher risk than adults in the research communities. Hence, the results were consistent with the study by Rinklebe et al., (2019) which looked at the hazards to adult and paediatric health from potentially hazardous compounds, and was re-stated by Gyamfi et al., (2021) who investigated was on contamination, exposure, and risk assessment of mercury in the soils of an artisanal gold mining community in Ghana.

CHAPTER FIVE

SUMMARY OF FINDINGS, RECOMMENDATIONS, AND CONCLUSION

The research was conducted to investigate the sources apportionment and human health risk assessment of potentially toxic elements (PTEs) in soil samples from artisanal small-scale mining areas in the Atwima Mponua district, Ghana. The study revealed critical insights into environmental contamination and associated health risks.

5.1 Summary of Findings

This study comprehensively assessed the levels, sources, and potential human health risks of potentially toxic elements (PTEs) in soils impacted by artisanal small-scale mining (ASGM) activities in the Atwima Mponua District of Ghana. Utilizing advanced analytical tec++hniques such as Positive Matrix Factorization (PMF), Principal Component Analysis (PCA), and various pollution indices, the study identified critical levels of contamination, particularly by cadmium (Cd) and cobalt (Co), which significantly exceed permissible limits and pose considerable ecological and human health risks

The analysis identified elevated levels of PTEs in decreasing order as follows: Fe >, Mn >, Cd >, Co >, Ti >, Zn >, Ni >, Cu >, As >, Pb >, V >, Cr >, and Hg. These elements are known for their detrimental effects on human health and the environment as a whole. The findings of this study show significant contamination of surface soils in the Atwima Mponua District, Ghana, due to artisanal small-scale mining (ASM) activities. Elevated concentrations of potentially toxic elements (PTEs), notably cadmium (Cd), cobalt (Co), and arsenic (As), exceed international soil quality benchmarks, highlighting critical environmental and public health concerns. Among the PTEs analyzed, Cd exhibited the

highest levels of contamination, enrichment, and ecological risk, accounting for over 99% of the total ecological risk index (PERI), a finding consistent with previous research in Ghanaian mining communities.

Soil pH, electrical conductivity (EC), and total organic carbon (TOC) assessments revealed acidic to neutral conditions with low organic matter content, which may facilitate metal mobility and bioavailability. The low TOC and moderate EC readings suggest the limited buffering capacity of the soil, likely increasing the risk of metal leaching into surrounding ecosystems and water bodies.

Spatial distribution maps further confirmed the widespread dispersion of Cd and Co across the study area, with high concentrations in regions proximate to mining hotspots. Pearson correlation and PCA confirmed strong associations between PTEs such as Ti, V, Cr, Cu, and Cd, indicating common origins, while negative associations between some variables point to differential mobility and retention in the soil, influenced by local physicochemical conditions.

Multivariate statistical analyses, including Principal Component Analysis (PCA) and Positive Matrix Factorization (PMF), effectively identified anthropogenic activities—particularly ASM and agriculture as the dominant sources of contamination. PMF identified five source profiles, with three (Factors 2, 4, and 5) linked primarily to anthropogenic influences, whereas the others reflected mixed geogenic and anthropogenic contributions. These analyses revealed a complex pattern of PTE origins, underscoring the interplay between lithogenic background and human activities in determining soil quality.

Importantly, the human health risk assessment revealed that both children and adults are at risk of non-carcinogenic effects, particularly via dermal contact and ingestion pathways. Children were found to be more vulnerable due to their physiological and behavioural characteristics. The hazard indices (HI) for children (35.89) and adults (6.30) exceeded the acceptable threshold (HI > 1), indicating high non-carcinogenic risks. While the total cancer risk (TCR) remained within acceptable limits, individual risks from As and Cd surpassed negligible levels, highlighting the long-term cancer potential associated with chronic exposure.

5.2 Conclusions

This study assessed the concentrations and ecological status of potentially toxic elements (PTEs) in surface soils of the Atwima Mponua District, Ghana, a region significantly impacted by artisanal small-scale mining (ASM) activities. The results revealed elevated levels of several PTEs, with the elements ranked in descending order of concentration as follows: Fe > Mn > Cd > Co > Ti > Zn > Ni > Cu > As > Pb > V > Cr > Hg. Among these, cadmium (Cd), cobalt (Co), and arsenic (As) were identified as the most critical contaminants due to their high ecological risk and enrichment values.

Quantitative analysis showed mean concentrations of Cd, Co, Mn, and As all exceeding international soil quality threshold limits. Cadmium posed the greatest threat, contributing over 99% to the Potential Ecological Risk Index (PERI). The enrichment factors (Erf) for Cd, Hg, and Co were all above 1.5, indicating significant anthropogenic influence, mainly from mining activities. The findings revealed that artisanal small-scale mining activities, serve as the primary anthropogenic contributors to soil contamination

in the study area. Geogenic factors were also identified as significant contributors to background PTE levels.

The spatial distribution analysis highlighted specific hotspots of pollution, emphasizing the urgent need for targeted remediation efforts. The results recognized the necessity for policy interventions, and sustainable mining practices to protect public health and preserve soil quality for future generations.

Correlation coefficient analyses suggested strong positive relationships among most PTEs, implying common sources primarily linked to ASM operations. These findings confirm severe environmental contamination and point to urgent public health risks within the district, particularly due to chronic exposure pathways such as ingestion and dermal contact

In this study, Positive Matrix Factorization (PMF) and Principal Component Analysis (PCA) were employed as advanced multivariate statistical tools to analysed and interpret the distribution and sources of potentially toxic elements (PTEs) in soils affected by artisanal small-scale mining (ASGM). These methods were pivotal in identifying pollution sources and understanding the extent of anthropogenic influence on soil quality. **PMF** was used for quantitative source apportionment, decomposing the complex dataset into source profiles and their relative contributions. The model effectively distinguished between natural (geogenic) and anthropogenic inputs, identifying ASGM activities as the dominant contributor to elevated levels of As, Mn, Ti, Hg, and Cd heavy metal(iod)s of which contributions exceeded internationally accepted soil contamination thresholds.

The output revealed multiple latent sources, including mining emissions, weathering of parent rock materials, and possibly agricultural inputs.

PCA was applied to reduce data dimensionality and explore correlations among PTEs. The analysis grouped elements based on similar variance structures, revealing strong associations among metals typically linked to mining processes. PCA also supported the differentiation of contamination origins, confirming the dominant anthropogenic footprint from ASGM operations.

The human health risk assessment showed that both children and adults in the region are exposed to non-carcinogenic and carcinogenic risks through ingestion, dermal contact, and inhalation pathways, with children being more vulnerable. This research not only fills an important knowledge gap regarding PTE contamination from ASGM in Ghana but also provides a scientific basis for informed decision-making and policy formulation. It is recommended that urgent mitigation strategies be implemented, including public education, land reclamation, stricter regulation of mining activities, and continuous environmental monitoring to reduce the risks associated with potentially toxic elements in the region.

5.3. Recommendations

Banning artisanal small-scale mining in Atwima Mponua District is not a feasible solution because it is currently a substantial source of income for the community. To lower the danger of disaster, this thesis recommends actions that can be employed.

There is the need for the government and local authorities to engage and collaborate with all stakeholders to formulate clear policies and disaster risk reduction measures for small-scale mining in the areas.

Further research is essential to investigate the high levels of cadmium, cobalt, arsenic, and manganese in the soil. This should focus on the bio-availability of these potentially toxic elements to better understand their impact on human health.

The application of positive matrix factorization (PMF) should be explored as a recommended approach to establish source profiles and source contributions of PTEs in the study area. This will aid in identifying specific pollution sources and developing target interventions.

It is crucial to raise awareness among residents of the Atwima Mponua District regarding the dangers associated with artisanal mining practices. Educational campaigns should discourage unsafe practices, such as forest mining, water buffers, and indiscriminate chemical applications.

REFERENCES

Aguilera, A., Bautista, F., Goguitchaichvili, A., & Garcia-oliva, F. (2021). Health Risk of Heavy Metals in Street Dust. *Frontiers in Bioscience, Landmark*, *26*(Jan), 327–345.

Alengebawy, A., Abdelkhalek, S. T., Qureshi, S. R., & Wang, M. Q. (2021). Heavy metals and pesticide toxicity in agricultural soil and plants: Ecological risks and human health implications. In *Toxics* (Vol. 9, Issue 3, pp. 1–34). MDPI AG. https://doi.org/10.3390/toxics9030042

Asamoah, B. D., Dodd, M., Yevugah, L. L., Borquaye, L. S., Boateng, A., Nkansah, M. A., & Darko, G. (2023a). Distribution and in-vitro bioaccessibility of potentially toxic metals in surface soils from a mining and a non-mining community in Ghana: implications for human health. *Environmental Geochemistry and Health*, *45*(12), 9875–9889. https://doi.org/10.1007/s10653-023-01776-5

Asamoah, B. D., Dodd, M., Yevugah, L. L., Borquaye, L. S., Boateng, A., Nkansah, M. A., & Darko, G. (2023b). Distribution and in-vitro bioaccessibility of potentially toxic metals in surface soils from a mining and a non-mining community in Ghana: implications for human health. *Environmental Geochemistry and Health*, *45*(12), 9875–9889. https://doi.org/10.1007/s10653-023-01776-5

Attachment 1-1 Guidance for Developing Ecological Soil Screening Levels (Eco-SSLs) Review of Existing Soil Screening Benchmarks. (2003).

Atwima Mponua DA. (2019). *Republic of Ghana Composite Budget for 2019-2022 Programme Based Budget Estimates for 2019 Atwima Mponua District Assembly*.

Brown, S. G., Eberly, S., Paatero, P., & Norris, G. A. (2015). Methods for estimating uncertainty in PMF solutions: Examples with ambient air and water quality data and guidance on reporting PMF results. *Science of the Total Environment*, *518–519*, 626–635. https://doi.org/10.1016/j.scitotenv.2015.01.022

Cipullo, S., Snapir, B., Tardif, S., Campo, P., Prpich, G., & Coulon, F. (2018). Insights into mixed contaminants interactions and its implication for heavy metals and metalloids mobility, bioavailability, and risk assessment. *Science of the Total Environment*, *645*, 662–673. https://doi.org/10.1016/j.scitotenv.2018.07.179

Circular on target values and intervention values for soil remediation. (n.d.-a). www.esdat.net

Coulter, C. T. (2004). *EPA-CMB8.2 User's Manual*.

Darko, G., Dodd, M., Nkansah, M. A., Ansah, E., & Aduse-Poku, Y. (2017). Distribution and bioaccessibility of metals in urban soils of Kumasi, Ghana. *Environmental Monitoring and Assessment*, *189*(6). https://doi.org/10.1007/s10661-017-5972-9

Dartey, E., & Gyamfi, O. (2024). Assessing Contamination Levels and Risk of Toxic Elements in Soils from Automobile Workshop Centre in Asante Mampong, Ghana. *Chemistry Africa*, *7*(2), 929–940. https://doi.org/10.1007/s42250-023-00799-w

Delower Hossain, Mir Mohammad Ali, & Maksuda Begum. (2020). Heavy Metals - Their Environmental Impacts and Mitigation. In *Heavy Metals - Their Environmental Impacts and Mitigation*. IntechOpen. https://doi.org/10.5772/intechopen.91574 *DOI: http://dx.doi.org/10.5772/intechopen.96805*

Donkor, A. K., Nartey, V. K., Bonzongo, J. C., & Adotey, D. K. (n.d.). Artisanal Mining of Gold with Mercury in Ghana. In *West Africa Journal of Applied Ecology* (Vol. 9). www.wajae.org

Epa, U., & Exposure Research Laboratory, N. (n.d.). *EPA Positive Matrix Factorization (PM F) 5.0 Fundamentals and User Guide*. www.epa.gov

Epa, U., & Factors Program, E. (n.d.). *Exposure Factors Handbook: 2011 Edition*. www.epa.gov

Fabiana Meijon Fadul. (2019). *Health risk of heavy metals in street dust Anahi* (Fourth Edi). CRC Press Taylor & Francis Group 6000 Broken Sound Parkway NW, Suite 300 Boca Raton, FL 33487-2742.

Final, I. (1989). *Risk Assessment: Guidance for Superfund Volume 1 Human Health Evaluation Manual (Part A)*. http://www.epa.gov/swerrims/riskassessment/risk_superfund.html

Fu, Y., Li, F., Guo, S., & Zhao, M. (2021). Cadmium concentration and its typical input and output fluxes in agricultural soil downstream of a heavy metal sewage irrigation area. *Journal of Hazardous Materials*, *412*. https://doi.org/10.1016/j.jhazmat.2021.125203

Ghana Statistical Service (GSS), GHANA 2021 POPULATION AND HOUSING CENSUS, Ghana Stat. Serv. VOLUME 3A (2021) 112. 〈https://census2021.statsghana.gov.gh/

Gold Mining Site, Southwest Nigeria. *Journal of the Geological Society of India*, *91*(6), 743–748. https://doi.org/10.1007/s12594-018-0933-7

Gündoğdu, A., Türk Çulha, S., & Koçbaş, F. (2020). Trace Elements Concentrations and Human Health Risk Evaluation for Four Common Fish Species in Sinop Coasts (Black Sea). *Turkish Journal of Agriculture - Food Science and Technology*, *8*(9), 1854–1862. https://doi.org/10.24925/turjaf.v8i9.1854-1862.3470

Gyamfi, O., Sørensen, P. B., Darko, G., Ansah, E., Vorkamp, K., & Bak, J. L. (2021). Contamination, exposure and risk assessment of mercury in the soils of an artisanal gold mining community in Ghana. *Chemosphere*, *267*. https://doi.org/10.1016/j.chemosphere.2020.128910

Gyamfi, O., Sorenson, P. B., Darko, G., Ansah, E., & Bak, J. L. (2020). Human health risk assessment of exposure to indoor mercury vapour in a Ghanaian artisanal small-scale gold mining community. *Chemosphere*, *241*. https://doi.org/10.1016/j.chemosphere.2019.125014

Hadzi, G. Y. (2017). *Assessment of Heavy Metals and Metalloids in Soils, Sediments and Water From Pristine and Major Mining Areas in Ghana - Data To Aid Geochemical Baseline Setting*. *October*.

Hayford, E. K., Amin, A., Osae, E. K., & Kutu, J. (2008). Impact of Gold Mining on Soil and some Staple Foods Collected from Selected Mining Communities in and around Tarkwa-Prestea Area. In *West African Journal of Applied Ecology* (Vol. 14).

Hossain Bhuiyan, M. A., Chandra Karmaker, S., Bodrud-Doza, M., Rakib, M. A., & Saha, B. B. (2021). Enrichment, sources, and ecological risk mapping of heavy metals in agricultural soils of Dhaka district employing SOM, PMF, and GIS methods. *Chemosphere*, *263*. https://doi.org/10.1016/j.chemosphere.2020.128339

https:// www. who. int/ news- room/ fact- sheets/ detail/obesi ty- and- overw eight. Accessed 31 May 2022 World Bank. (2020). *Ghana: Country Environmental Analysis*.

Jaishankar, M., Tseten, T., Anbalagan, N., Mathew, B. B., & Beeregowda, K. N. (2014). Toxicity, mechanism, and health effects of some heavy metals. In *Interdisciplinary Toxicology* (Vol. 7, Issue 2, pp. 60–72). Slovak Toxicology Society. https://doi.org/10.2478/intox-2014-0009

Kabir, H., & Rashid, H. (2022). Estimation of Pollution Levels and Assessment of Human Health Risks from Potentially Toxic Metals in Road Dust in. *Processes*, *10*(2474), https://doi.org/10.3390/ pr10122474.

Kamunda, C., Mathuthu, M., & Madhuku, M. (2016). Health risk assessment of heavy metals in soils from Witwatersrand gold mining basin, South Africa. *International Journal of Environmental Research and Public Health*, *13*(7). https://doi.org/10.3390/ijerph13070663

Konadu, F. N., Gyamfi, O., Ansah, E., Borquaye, L. S., Agyei, V., Dartey, E., Dodd, M., Obiri-Yeboah, S., & Darko, G. (2023). Human health risk assessment of potentially toxic elements in soil and air particulate matter of automobile hub environments in Kumasi, Ghana. *Toxicology Reports*, *11*, 261–269. https://doi.org/10.1016/j.toxrep.2023.09.010

Kumar, V., Parihar, R. D., Sharma, A., Bakshi, P., Singh Sidhu, G. P., Bali, A. S., Karaouzas, I., Bhardwaj, R., Thukral, A. K., Gyasi-Agyei, Y., & Rodrigo-Comino, J. (2019). Global evaluation of heavy metal content in surface water bodies: A meta-analysis using heavy metal pollution indices and multivariate statistical analyses. In *Chemosphere* (Vol. 236). Elsevier Ltd. https://doi.org/10.1016/j.chemosphere.2019.124364

Mackey, E. A., Greenberg, R. R., & Wise, S. A. (2009a). *Standard Reference Material ® 2711a Montana II Soil Moderately Elevated Trace Element Concentrations Measurement Services Division*.

Mensah, A. K., Marschner, B., Antoniadis, V., Stemn, E., Shaheen, S. M., & Rinklebe, J. (2021). Human health risk via soil ingestion of potentially toxic elements and remediation potential of native plants near an abandoned mine spoil in Ghana. *Science of the Total Environment*, *798*. https://doi.org/10.1016/j.scitotenv.2021.149272

Mkhize, T. A. (2020). *Assessment of heavy metal contamination in soils around Krugersdorp mining area*.

Naqvi, S. A. R., Idrees, F., Sherazi, T. A., Shahzad, S. A., Hassan, S. U. L., & Ashraf, N. (2022). Toxicology of Heavy Metals Used in Cosmetics. *Journal of the Chilean Chemical Society*, *67*(3), 5615–5622. https://doi.org/10.4067/S0717-97072022000305615

Nkansah, M. A., Darko, G., Dodd, M., Opoku, F., Bentum Essuman, T., & Antwi-Boasiako, J. (2017). Assessment of pollution levels, potential ecological risk and human health risk of heavy metals/metalloids in dust around fuel filling stations from the Kumasi Metropolis, Ghana. *Cogent Environmental Science*, *3*(1). https://doi.org/10.1080/23311843.2017.1412153

Odukoya, A. M., Olobaniyi, S. B., & Oluseyi, T. O. (2018). Assessment of Potentially Toxic Elements Pollution and Human Health Risk in Soil of Ilesha

Paatero, P., Eberly, S., Brown, S. G., & Norris, G. A. (2014). Methods for estimating uncertainty in factor analytic solutions. *Atmospheric Measurement Techniques*, *7*(3), 781–797. https://doi.org/10.5194/amt-7-781-2014

Polissar, A. V., Hopke, P. K., Paatero, P., Malm, W. C., & Sisler, J. F. (1998). Atmospheric aerosol over Alaska 2. Elemental composition and sources. *Journal of Geophysical Research Atmospheres*, *103*(D15), 19045–19057. https://doi.org/10.1029/98JD01212

Proshad, R., Islam, M. S., Kormoker, T., Sayeed, A., Khadka, S., & Idris, A. M. (2021). Potential toxic metals (PTMs) contamination in agricultural soils and foodstuffs with associated source identification and model uncertainty. *Science of the Total Environment*, *789*. https://doi.org/10.1016/j.scitotenv.2021.147962

Qin, G., Niu, Z., Yu, J., Li, Z., Ma, J., & Xiang, P. (2021). Soil heavy metal pollution and food safety in China: Effects, sources and removing technology. In *Chemosphere* (Vol. 267). Elsevier Ltd. https://doi.org/10.1016/j.chemosphere.2020.129205

Rabin, M. H., Wang, Q., Kabir, M. H., & Wang, W. (2023). Pollution characteristics and risk assessment of potentially toxic elements of fine street dust during COVID-19 lockdown in Bangladesh. *Environmental Science and Pollution Research*, *30*(2), 4323–4345. https://doi.org/10.1007/s11356-022-22541-8

Rinklebe, J., Antoniadis, V., Shaheen, S. M., Rosche, O., & Altermann, M. (2019). Health risk assessment of potentially toxic elements in soils along the Central Elbe River, Germany. *Environment International*, *126*, 76–88. https://doi.org/10.1016/j.envint.2019.02.011

Risk Assessment. *United States Environmental Protection Agency*, 1–20. https://www.epa.gov/risk/conducting-human-health-risk-assessment

Song, J., Liu, Q., & Sheng, Y. (2019). Distribution and risk assessment of trace metals in riverine surface sediments in gold mining area. *Environmental Monitoring and Assessment*, *191*(3). https://doi.org/10.1007/s10661-019-7311-9

Update. (1999). *Canadian Environmental Quality Guidelines Canadian Council of Ministers of the Environment Canadian Soil Quality Guidelines for the Protection of Environmental and Human Health SUMMARY TABLES*. http://www.ccme.ca/publications/ceqg_rcqe.html?category_id=125] venti on-values- 2000- esdat. Accessed 27 May 2022

VROM. (2000). Dutch Target and Intervention Values; 2000 (the New Dutch List). *Netherlands Government Gazette*, *2000*(4th February, 2000), 1–12. https:// www. yumpu.com/ en/ docum ent/ view/ 44815 398/ dutch- target- and- inter

Washington DC 20433. https:// docum ents1. world bank.org/ curat ed/ en/ 41987 15885 78973 802/ pdf/ Ghana- Country- Envir onmen tal- Analy sis. pdf. Accessed 31 May 2022 https://doi.org/10.1016/j.toxrep.2023.09.010

WHO Global Strategy on Health, Environment and Climate Change. (2020). http://apps.who.int/bookorders.

WHO. (2021). *Obesity and overweight*. Geneva 27, Switzerland.

Yang, J., Sun, Y., Wang, Z., Gong, J., Gao, J., Tang, S., Ma, S., & Duan, Z. (2022). Heavy metal pollution in agricultural soils of a typical volcanic area: Risk assessment and source appointment. *Chemosphere*, *304*. https://doi.org/10.1016/j.chemosphere.2022.135340

WHO. (2021). *Obesity and overweight*. Geneva 27, Switzerland.https:// www. who. int/ news- room/ fact- sheets/ detail/obesi ty- and- overw eight. Accessed 31 july, 2024.

Zhao, C., Yang, J., Zhang, X., Fang, X., Zhang, N., Su, X., Pang, H., Li, W., Wang, F., Pu, Y., & Xia, Y. (2023). A human health risk assessment of rare earth elements through daily diet consumption from Bayan Obo Mining Area, China. *Ecotoxicology and Environmental Safety*, *266*(October), 115600. https://doi.org/10.1016/j.ecoenv.2023.115600

APPENDICES

Appendix 1. table of the Scope Area of Study

ID	Latitude	Longitude	ID	Latitude	Longitude	ID	Latitude	Longitude
AMP 001	6.7815	-2.02717	AAM 032	6.61825	-1.99381	NKA 058	6.61825	-1.99381
AMP 002	6.7815	-2.02717	AAM 033	6.61825	-1.99381	NKA 059	6.61825	-1.99381
AMP 003	6.61625	-1.99197	AAM 034	6.61825	-1.99381	NKA 060	6.61825	-1.99381
AMP 004	6.624333	-1.97822	AAM 35	6.61825	-1.99381	NKA 061	6.61825	-1.99381
AMP 005	6.624333	-1.97822	AAM 036	6.61825	-1.99381	NKA 062	6.61825	-1.99381
AAP 006	6.697	-1.54158	AAM 037	6.61825	-1.99381	NKA 063	6.61825	-1.99381
AMP 007	6.697	-1.54158	AAM 038	6.61825	-1.99381	NKA 064	6.61825	-1.99381
AMP 008	6.702333	-1.74156	APA 039	6.61825	-1.99381	NKA 065	6.61825	-1.99381
AMP 009	6.61825	-1.97714	APA 040	6.61825	-1.99381	NKA 066	6.61825	-1.99381
AMP 010	6.61825	-1.99381	APA 041	6.620417	-1.03419	NKA 067	6.61825	-1.99381
AMP 011	6.61825	-1.99381	APA 042	6.620417	-1.03419	NKA 068	6.61825	-1.99381
AMP 012	6.620417	-2.03419	APA 043	6.61825	-1.99381	NKA 069	6.61825	-1.99381
AMP 013	6.61825	-1.99381	APA 044	6.61825	-1.99381	NKA 070	6.61825	-1.99381
AMP 014	6.61825	-1.99381	APA 046	6.609111	-2.06419	NKA 071	6.61825	-1.99381
AMP 017	6.61825	-1.99381	APA 047	6.61825	-1.99381	NKA 072	6.61825	-1.99381
AMP 019	6.61825	-1.99381	APA 048	6.61825	-1.99381	NKA 073	6.61825	-1.99381
AMP 020	6.61825	-1.99381	APA 049	6.620417	-2.03419	UKA 074	6.61825	-1.99381
AMP 021	6.61825	-1.99381	APA 050	6.620417	-2.03419	UKA 075	6.61825	-1.99381
AMP 023	6.61825	-1.99381	APA 051	6.61825	-1.99381	KKA 076	6.61825	-1.99381
AAM 027	6.61825	-1.99381	NKA 052	6.700972	-1.75342	KKA 077	6.61825	-1.99381
AAM 028	6.675417	-1.97578	NKA 053	6.61825	-1.99381	KKA 078	6.620417	-1.99381
AAM 029	6.61825	-1.99381	NKA 054	6.61825	-1.99381	KKA 079	6.620417	-1.99381
AAM 030	6.61825	-1.99381	NKA 055	6.61825	-1.99381			
AAM 031	6.61825	-1.99381	NKA 057	6.61825	-1.99381			

Appendix 2 table showing the calculations of Cancer Risk for PTEs in Soil

Cancer Slope Factor (mg/(kgd)-CHILDREN										
Elements	BDIing	CSFing	Cancer Risk	BDIinh	CSFinh	Cancer Risk	BDIderm	Sfderm	Cancer Risk	mean
As	2.56E-05	1.5	3.84E-05	1.03E-15	1.50E+01	1.54E-14	2.43E-07	3.66E+00	8.88E-07	1.31E-05
Cd	0	0	0	2.60E-14	6.3	1.64E-13	6.16E-06	2.00E+01	1.23E-04	4.11E-05
Cr	3.35E-06	5.00E-01	1.68E-06	6.13E-17	4.02	2.47E-16	1.45E-08	2.00E+01	2.90E-07	6.56E-07
Pb	3.46E-06	8.50E-03	2.94E-08	5.80E-16	4.20E-02	2.44E-17	1.38E-07	0	0.00E+00	9.80E-09
										5.48E-05
Cancer Slope Factor (mg/(kgd) –_ DULTS										
Elements	BDIing	CSFing		BDIinh	CSFinh		BDIderm	CSFderm	Cancer Risk	mean
As	5.49E-06	1.5	8.23E-06	1.32E-15	15	1.98E-14	3.82E-08	3.66	1.40E-07	2.79E-06
Cd	0	0	0	3.35E-14	6.3	2.11E-13	9.71E-07	20	1.94E-05	6.47E-06
Cr	7.18E-07	0.5	3.59E-07	7.89E-17	4.02	3.17E-16	2.29E-09	20	4.58E-08	1.35E-07
Pb	1.48E-06	0.0085	1.26E-08	7.46E-16	0.042	3.13E-17	2.17E-08	0	0.00E+00	4.20E-09
										9.40E-06

Appendix 3. table of estimated for Hg HQ and HI for Children and Adults in 4 pathways

ID	HQing_A	HQing_C	HQinh_A	HQinh_C	HQder_A	HQder_C	HQvap_A	HQvap_C	HI_A	HI_C
GS182	0.000571	0.005328	1.56E-07	2.77E-07	3.31E-05	0.000217	0.00656	0.011633	0.007164	0.017178
GS183	0.000733	0.006846	2.01E-07	3.56E-07	4.26E-05	0.000279	0.00843	0.014949	0.009206	13.32603
GS184	0.000118	0.001103	3.23E-08	5.73E-08	6.86E-06	4.49E-05	0.001358	0.002408	0.001483	0.003556
GS185	0.000149	0.001388	4.07E-08	7.21E-08	8.63E-06	5.65E-05	1.71E-03	3.03E-03	0.001866	0.004475
GS186	0.000611	0.0057	1.67E-07	2.96E-07	3.54E-05	2.32E-04	7.02E-03	1.24E-02	0.007665	0.018379
GS187	0.000394	0.003676	1.08E-07	1.91E-07	2.29E-05	1.50E-04	4.53E-03	8.03E-03	0.004943	0.011852
GS188	0.000186	0.001737	5.09E-08	9.03E-08	1.08E-05	7.07E-05	2.14E-03	3.79E-03	0.002335	0.0056
GS189	0.000611	0.0057	1.67E-07	2.96E-07	3.54E-05	2.32E-04	7.02E-03	0.012446	0.007665	0.018379
GS190	3.94E-05	0.000368	1.08E-08	1.91E-08	2.29E-06	1.50E-05	4.53E-04	0.000803	0.000494	0.001185
GS191	0.000186	0.001737	5.09E-08	9.03E-08	1.08E-05	7.07E-05	2.14E-03	0.003792	0.002335	0.0056
GS192	0.000105	0.000978	2.87E-08	5.08E-08	6.08E-06	3.98E-05	1.20E-03	0.002135	0.001315	0.003152
GS193	4.42E-05	0.000413	1.21E-08	2.15E-08	2.57E-06	1.68E-05	5.08E-04	0.000902	0.000555	0.001331

GS194	0.000339	0.003162	9.27E-08	1.64E-07	1.97E-05	1.29E-04	3.89E-03	0.006904	0.004252	0.010195
GS195	0.00021	0.001963	5.75E-08	1.02E-07	1.22E-05	8.00E-05	2.42E-03	0.004287	0.00264	0.00633
GS196	0.000124	0.001156	3.39E-08	6.01E-08	7.19E-06	4.71E-05	1.42E-03	0.002524	0.001555	0.003728
GS197	0.000337	0.003144	9.22E-08	1.63E-07	1.96E-05	0.000128	0.003872	0.006866	0.004228	0.010139
GS198	0.000404	0.003766	1.1E-07	1.96E-07	2.34E-05	0.000153	0.004638	0.008224	0.005065	0.012144
GS199	0.000421	0.003929	1.15E-07	2.04E-07	2.44E-05	0.00016	0.004838	0.008579	0.005283	0.012668
GS200	0.000278	0.002594	7.61E-08	1.35E-07	1.61E-05	0.000106	0.003195	0.005665	0.003489	0.008365
GS201	0.000182	0.001702	4.99E-08	8.85E-08	1.06E-05	6.93E-05	0.002096	0.003717	0.002289	0.005488
GS202	0.000188	0.001755	5.15E-08	9.12E-08	1.09E-05	7.15E-05	0.002161	0.003833	0.002361	0.00566
GS203	0.000165	0.001537	4.51E-08	7.99E-08	9.56E-06	6.26E-05	0.001892	0.003356	0.002067	0.004956
GS204	0.000181	0.001689	4.95E-08	8.78E-08	1.05E-05	6.88E-05	0.002079	0.003687	0.002271	0.005445
GS205	0.000264	0.002461	7.21E-08	1.28E-07	1.53E-05	0.0001	0.003031	0.005374	0.00331	0.007936
GS206	0.000132	0.001236	3.62E-08	6.42E-08	7.69E-06	5.03E-05	0.001522	0.002699	0.001662	0.003985
GS207	0.000231	0.002158	6.32E-08	1.12E-07	1.34E-05	8.79E-05	0.002657	0.004711	0.002901	0.006957

GS207	0.000231	0.002158	6.32E-08	1.12E-07	1.34E-05	8.79E-05	0.002657	0.004711	0.002901	0.006957
GS208	0.000177	0.001652	4.84E-08	8.59E-08	1.03E-05	6.73E-05	0.002034	0.003607	0.002221	0.005326
GS209	0.000491	0.004581	1.34E-07	2.38E-07	2.85E-05	0.000187	0.005641	0.010004	0.006161	0.014771
GS210	0.000235	0.002197	6.44E-08	1.14E-07	1.37E-05	8.95E-05	0.002706	0.004798	0.002955	0.007086
GS211	0.000259	0.002421	7.1E-08	1.26E-07	1.51E-05	9.86E-05	0.002981	0.005287	0.003256	0.007807
GS212	0.000439	0.004102	1.2E-07	2.13E-07	2.55E-05	0.000167	0.005051	0.008957	0.005516	0.013226
GS213	2.23E-05	0.000208	6.09E-09	1.08E-08	1.29E-06	8.46E-06	0.000256	0.000454	0.000279	0.00067
GS214	0.000207	0.001931	5.66E-08	1E-07	1.2E-05	7.87E-05	0.002378	0.004217	0.002597	0.006227
GS215	0.00028	0.002617	7.67E-08	1.36E-07	1.63E-05	0.000107	0.003222	0.005715	0.003519	0.008438
GS216	6.08E-05	0.000567	1.66E-08	2.95E-08	3.53E-06	2.31E-05	0.000699	0.001239	0.000763	0.001829
GS217	4.11E-05	0.000384	1.12E-08	1.99E-08	2.39E-06	1.56E-05	0.000472	0.000838	0.000516	0.001237
GS218	6.76E-05	0.000631	1.85E-08	3.28E-08	3.93E-06	2.57E-05	0.000777	0.001378	0.000849	0.002035
GS219	8.82E-05	0.000823	2.41E-08	4.28E-08	5.12E-06	3.35E-05	0.001013	0.001797	0.001107	0.002654
GS220	0.003996	0.037293	1.09E-06	1.94E-06	0.000232	0.001519	0.045922	0.081434	0.05015	0.120249
GS221	0.000377	0.003519	1.03E-07	1.83E-07	2.19E-05	0.000143	0.004333	0.007683	0.004732	0.011345

GS222	9.3E-05	0.000868	2.55E-08	4.51E-08	5.4E-06	3.54E-05	0.001069	0.001896	0.001168	0.0028
GS223	0.00032	0.002983	8.74E-08	1.55E-07	1.85E-05	0.000121	0.003673	0.006514	0.004011	0.009618
GS224	0.000674	0.006286	1.84E-07	3.27E-07	3.91E-05	0.000256	0.007741	0.013727	0.008454	0.02027
GS225	0.000654	0.006099	1.79E-07	3.17E-07	3.79E-05	0.000248	0.007511	0.013319	0.008202	0.019667
GS226	0.000425	0.003969	1.16E-07	2.06E-07	2.47E-05	0.000162	0.004887	0.008667	0.005337	0.012798
GS227	0.000397	0.003702	1.09E-07	1.92E-07	2.3E-05	0.000151	0.004559	0.008084	0.004979	0.011937
GS228	0.000128	0.001199	3.51E-08	6.23E-08	7.45E-06	4.88E-05	0.001476	0.002617	0.001612	0.003865
GS229	0.000776	0.007245	2.12E-07	3.77E-07	4.51E-05	0.000295	0.008922	0.015821	0.009743	0.023362
GS230	0.000277	0.002584	7.57E-08	1.34E-07	1.61E-05	0.000105	0.003181	0.005642	0.003474	0.008331
GS231	0.00015	0.001396	4.09E-08	7.26E-08	8.68E-06	5.69E-05	0.001719	0.003049	0.001878	0.004503
GS232	0.000218	0.002032	5.96E-08	1.06E-07	1.26E-05	8.28E-05	0.002503	0.004438	0.002733	0.006553
GS233	0.000108	0.001009	2.96E-08	5.25E-08	6.28E-06	4.11E-05	0.001243	0.002204	0.001358	0.003255
GS234	9.33E-05	0.000871	2.55E-08	4.53E-08	5.42E-06	3.55E-05	0.001073	0.001902	0.001171	0.002808
GS235	0.000479	0.004475	1.31E-07	2.33E-07	2.78E-05	0.000182	0.00551	0.009771	0.006018	0.014429
GS236	0.000773	0.007218	2.12E-07	3.75E-07	4.49E-05	0.000294	0.008888	0.015762	0.009707	0.023274

GS237	0.000169	0.001577	4.62E-08	8.2E-08	9.81E-06	6.42E-05	0.001942	0.003443	0.00212	0.005084
GS238	0.000324	0.003023	8.86E-08	1.57E-07	1.88E-05	0.000123	0.003723	0.006601	0.004065	0.009748
GS239	0.000676	0.006313	1.85E-07	3.28E-07	3.93E-05	0.000257	0.007773	0.013785	0.008489	0.020355
GS240	0.000565	0.005274	1.55E-07	2.74E-07	3.28E-05	0.000215	0.006494	0.011516	0.007092	0.017005
GS241	0.000514	0.004795	1.41E-07	2.49E-07	2.98E-05	0.000195	0.005904	0.010469	0.006447	0.015459
GS242	0.000839	0.007831	2.3E-07	4.07E-07	4.87E-05	0.000319	0.009643	0.0171	0.010531	0.02525
GS243	0.000848	0.007911	2.32E-07	4.11E-07	4.92E-05	0.000322	0.009741	0.017275	0.010638	0.025508
GS244	0.000107	0.000999	2.93E-08	5.19E-08	6.21E-06	4.07E-05	0.00123	0.002181	0.001343	0.003221
GS245	0.000132	0.001231	3.61E-08	6.4E-08	7.65E-06	5.01E-05	0.001515	0.002687	0.001655	0.003968
GS246	0.000116	0.001079	3.16E-08	5.61E-08	6.71E-06	4.39E-05	0.001328	0.002356	0.001451	0.003478
GS247	0.000156	0.001454	4.26E-08	7.56E-08	9.04E-06	5.92E-05	0.001791	0.003176	0.001956	0.004689
GS248	0.000133	0.001239	3.63E-08	6.44E-08	7.7E-06	5.04E-05	0.001525	0.002705	0.001666	0.003994
GS249	0.000158	0.00147	4.31E-08	7.64E-08	9.14E-06	5.99E-05	0.00181	0.003211	0.001977	0.004741
GS250	0.000351	0.003276	9.6E-08	1.7E-07	2.04E-05	0.000133	0.004034	0.007154	0.004406	0.010564
GS251	0.000133	0.001239	3.63E-08	6.44E-08	7.7E-06	5.04E-05	0.001525	0.002705	0.001666	0.003994
GS252	0.000745	0.006952	2.04E-07	3.61E-07	4.32E-05	0.000283	0.008561	0.015181	0.009349	0.022416

GS253	0.000445	0.004155	1.22E-07	2.16E-07	2.58E-05	0.000169	0.005117	0.009073	0.005588	0.013398
GS254	0.000164	0.001534	4.5E-08	7.98E-08	9.54E-06	6.25E-05	0.001889	0.00335	0.002063	0.004947
GS255	0.000109	0.001015	2.97E-08	5.28E-08	6.31E-06	4.13E-05	0.00125	0.002216	0.001365	0.003272
GS256	0.000331	0.003092	9.07E-08	1.61E-07	1.92E-05	0.000126	0.003808	0.006753	0.004159	0.009971
GS257	0.000241	0.002253	6.61E-08	1.17E-07	1.4E-05	9.18E-05	0.002775	0.004921	0.00303	0.007266
GS258	0.00017	0.001586	4.65E-08	8.25E-08	9.86E-06	6.46E-05	0.001953	0.003464	0.002133	0.005114
GS259	0.000402	0.003748	1.1E-07	1.95E-07	2.33E-05	0.000153	0.004615	0.008184	0.00504	0.012084
MEAN	0.00035	0.003271	9.59E-08	1.7E-07	2.03E-05	0.000133	0.004028	0.007142	0.004399	0.18111
									0.343092	14.12661

Appendix 4. Summary Erf and CF reference Interpretation values for PTEs in Soil (Konadu et al., 2023)

Enrichment factor	**Risk category**
EF<2	Deficiency to minimal enrichment
2<EF<5	Moderate enrichment
5<EF<20	Significant enrichment
20<EF<40	Very high enrichment
EF>40	Extremely high enrichment
Contamination factor	**Contamination level**
CF<1	Low contamination
1 ≤ Cf< 2	Low to moderate contamination
2≤CF<3	Moderate contamination
3≤ Cf< 4	Moderate to high contamination
4 ≤ Cf< 5	High contamination
5≤CF<6	High to very high contamination
CF>6	Extreme contamination

Appendix 5. Summary of Some International background values for Toxic Elements in Soil (Brown et al., 2015)

PDM (mg/kg)	FAO/WHO Std.	VROM 2000 Target val.	EU Std.	CCM Std.	SOUTH AFRICA	CRUSTAL Avg.	USEPA	NIST SRM 2711b
Cu	100	36	140	91	16	25	>50	140 ± 2
Pb	100	85	300	260	20	17	>60	
Zn	300	140	300	360	240	71	>200	414 ± 11
Ni	50	35	75	50	91	44		21.7 ± 0.7
Co	50	9		300	300	17		9.89 ± 0.18
Fe						35		
As	1.5	29		12	5.8	1.5		107 ± 1.4
Cd	3	0.8	3	22	7.5	0.1	>200	54.1 ± 0.5
Mn						600		675 ± 18
Hg	0.5	0.3		24			0.5	
Ti				300				
Cr	100	100	100	87	6.5	83	>75	52.3 ± 2.9
V		42						80.7 ± 5.7
pH				6 to 8				

FAO/WHO Guidelines- Chiroma et al., 2014: Dutch International Values (VROM, 2000): EU Guidelines – European Commission on the environment, 2002: Canadian Council of Ministers of the Environment (CCME) soil quality guidelines (CCME, 2007): South Africa Guidelines -Dept. of envtal. Affairs, 2010: Crustal Avg(Odukoya et al., 2018): USEPA (Naqvi et al., 2022): NIST (SRM 2711)(Mackey et al., 2009)